ROOF SYSTEMS BEHAVIOR

Progress Report

EXPERIMENTAL STUDIES OF Z-PURLIN SUPPORTED ROOF SYSTEMS USING QUARTER SCALE MODELS

by

Venkatesh Seshappa

and

Thomas M. Murray
Principal Investigator

Sponsored by

Metal Building Manufacturers Association
and
American Iron and Steel Institute

Report No. FSEL/MBMA 85-02

May 1985

FEARS STRUCTURAL ENGINEERING LABORATORY
School of Civil Engineering and Environmental Science
University of Oklahoma
Norman, Oklahoma 73019

ACKNOWLEDGEMENTS

The research reported here was sponsored by the Metal Building Manufacturers Association and by the American Iron and Steel Institute under the guidance of the MBMA Roof Systems Behavior Research Subcommittee. Material for the test specimens was supplied by Star Manufacturing Company.

The contents of this report are essentially the same as the thesis submitted by Venkatesh Seshappa to the faculty of the School of Civil Engineering and Environmental Science, University of Oklahoma, in partial fulfillment of the requirements for the degree of Master of Science.

TABLE OF CONTENTS

LIST OF FIGURES

LIST OF TABLES

EXPERIMENTAL STUDIES OF Z-PURLIN SUPPORTED ROOF SYSTEMS USING QUARTER SCALE MODELS

CHAPTER I

INTRODUCTION

1.1 Definition of Problem

Cold-formed steel structural members are commonly used, particularly by the metal building industry, to support roof loads. Typically, roof panels are fastened to the cold-formed steel structural member using self-drilling or self-tapping fasteners. This type of roof system is referred to as a "thru-fastener" system.

The most widely used cold-formed steel members are of C-shape or Z-shape. These sections are usually cold-form fabricated from steel sheets, strips or plates either in roll-forming machines, or by press brake or bending brake operations. The edges of the flanges are "lipped" for stiffening as shown in Figure 1.1. These edge stiffeners or "lips" significantly increase the axial compression strength (local buckling strength) of the flanges.

The advantages of Z- and C-sections are that they are light, easy to fabricate and mass produce, allow fast and easy erection and are generally economical. However,

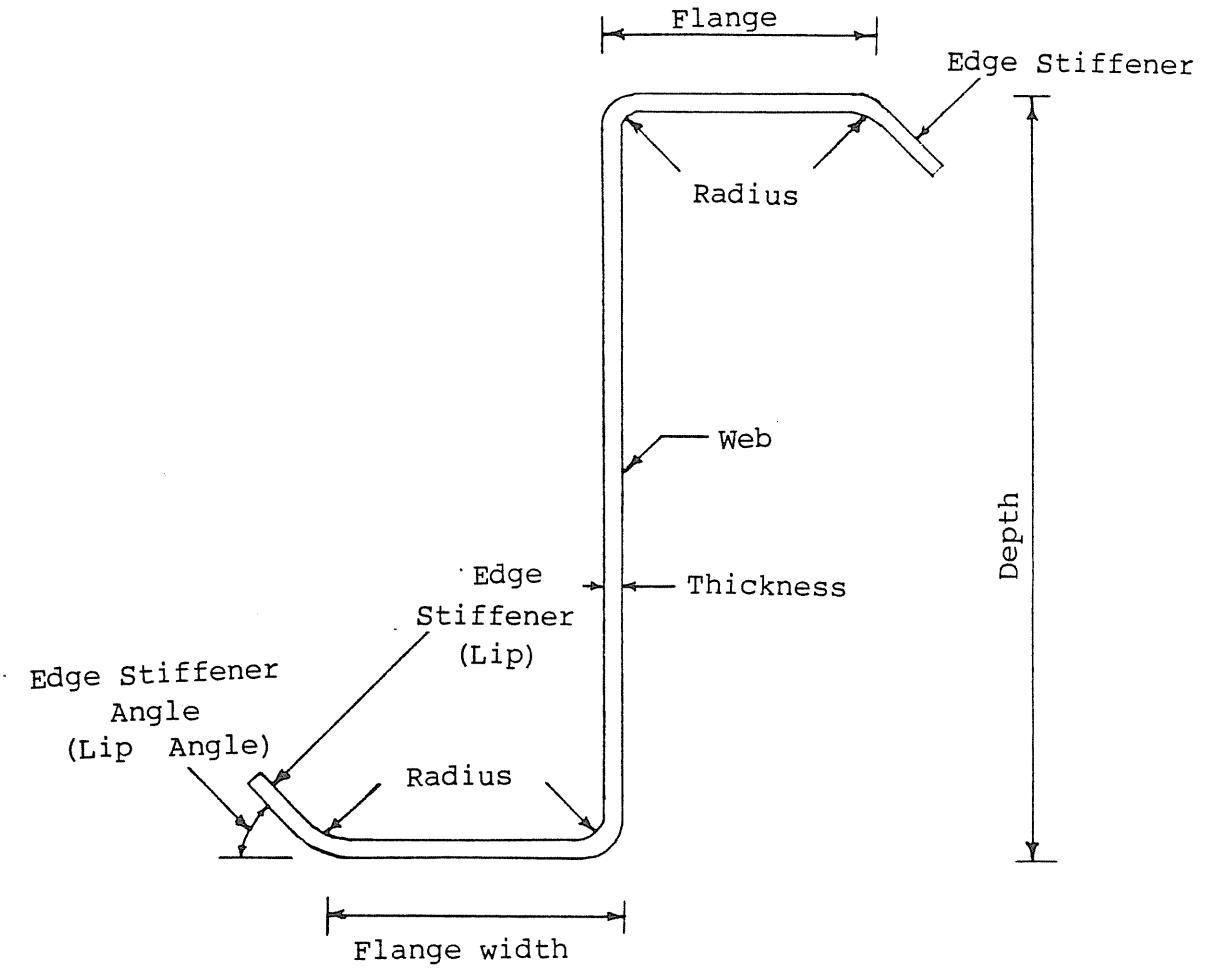

Figure 1.1 Cold-Formed Z-Purlin Geometry

because the line of action of the supported load does not pass through the shear center of C-sections or is not parallel to Z-section principal axes, the members tend to twist and/or move laterally as the loading is increased. If this movement is unrestrained the load carrying capacity of the member is greatly reduced. Thus, to fully develop or at least to improve the load carrying capacity of a cold-formed Z- or C-section, lateral and/or torsional restraint must be provided in the structural system.

The magnitude of the restraint force to develop the full flexural capacity of a member is much greater, 2 to 3 times, for a Z-purlin than for a C-purlin. The AISI "Specification for the Design of Cold-Formed Members" [1] suggests a procedure to estimate the forces developed in discrete brace systems where both the top and bottom flanges are fully restrained from lateral movement. However, the more common case where restraint is only provided at one flange (usually the top flange) is not mentioned in this specification. The possibility that system effects occur, that is, that the force required to restrain a number of purlin lines is less than that required to restrain the same number of individual members, is also not discussed.

From previous studies at the University of Oklahoma [2, 3, 4, 5], it is known that: (i) the magnitude of restraint forces in typical thru fastener roof systems are not as large as predicted by the AISI specification method and (ii) that the forces decrease, as a percent of total applied loading, with increasing number of purlin lines. The purpose of the experimental research reported here and of a sister analytical study was to prove or disprove the above contentions.

In the following section, previous analytical and experimental works concerning restraint forces in thru fastener, Z-purlin supported roof systems are reviewed.

1.2 Review of Previous Research

1.2.1 Previous Analytical Work

Zetlin and Winter [6] were the first to study the problem of lateral restraint forces for Z-purlins. They used simple bending equations and concluded that, if the unbraced length is large, second order effects (P-Δeffects) cannot be neglected. They suggested that the intermediate braces must be used to achieve the maximum load capacity of the members. Then, they developed a numerical procedure to determine deflection and stresses in intermediately braced Z-sections using a modified moment of inertia approach. However, their procedure cannot be used to analyze and design the roof system, as it is valid only for a single member with discrete or continuous braces attached to both flanges.

Needham [7] conducted several two purlin line roof system tests with a roof slope of 1/2:12. Based on limited test results, he developed a mathematical model for Z-purlin supported roof systems with the following assumptions: (i) simple beam supports; (ii) purlin clips that resist rotation but not warping; and (iii) no lateral intermediate braces. Based on his model, he suggested a design procedure to calculate panel diaphragm loads. His model does not consider intermediate braces nor continuous purlin systems. In his recommendations for future research, he suggested studying the influence of purlin

bridging on panel loads and purlin behavior and the relationship between the stiffness of the panel restraining system and the load transferred to it.

Ghazanfari and Murray [5] considered some of the above parameters. They conducted a number of full scale tests and based on the test results, they developed a more realistic design procedure. However, they only considered two purlin line, single span roof systems but with different lateral restraint conditions. The design procedure suggested by them considers the warping and second order effects and permits the calculation of restraining forces developed in several lateral restraint systems. Their design procedure is applicable only to two purlin line, single span systems. In the above reference computer programs are given to calculate the restraining forces.

1.2.2 Previous Experimental Work

As mentioned earlier, Needham [7] conducted a limited number of tests on full scale roof systems to study the behavior of such systems. Each of his test assemblies consisted of roof panels fastened to two 9.5 in. deep purlins spaced at 5 ft. on center. Lateral restraint was provided at two discrete locations along the span, one at each end of the span. The forces developed at these two locations were measured using load cells. Simulated gravity load was applied using concrete bricks and horizontal and vertical deflections were measured. The measured lateral loads in two tests were 9.1% and 9.7% of the total load.

Ghazanfari and Murray [2, 3, 5] conducted nine single span, two purlin line tests with four different lateral

bracing configurations. Seven tests at 19.625 ft. span were loaded to failure; one test at 22.5 ft. span and one test at 14.625 ft. span were not loaded to failure. The restraint conditions were: (i) torsional restraint at rafters; (ii) intermediate braces at midspan and quarter points; (iii) combination of (i) and (ii); and (iv) lateral braces at every 2 ft. with torsional restraint. The measured lateral force for configuration (i) varied between 21.0% and 28.5% of the total supported load, and that for configuration (ii), between 14.4% and 21.3% of the total supported vertical load. The measured lateral force varied between 19.3% and 22.5% of the total vertical load for configuration (iii), and for configuration (iv), between 14.1% and 16.1% of the total supported vertical load.

Curtis and Murray [4] studied the behavior of single span multiple Z-purlin line roof systems. Their study was limited to torsional brace force configurations and in-plane stiffness of such systems. In their report, they summarized the results of twenty gravity load tests of two, six and seven purlin line systems and nine stiffness tests of two and seven purlin line systems. They concluded that increasing the number of purlin lines in a system decreases the brace force from 5% to 10% when measured as a percent of total applied load.

Curtis and Murray also studied the behavior of three span, two purlin line systems. (Their results have not been published, however, their data was made available for comparison in Chapter 4). Two tests were conducted with zero roof slope and one test with a roof slope of 1/2:12. In all tests, lateral restraints were provided at the rafters and simulated gravity loading was applied using concrete blocks.

The full scale tests conducted by the above researchers have provided valuable information on the behavior of the type of roof systems under study here. However, the information obtained is not conclusive and additional testing of roof systems is needed to better define system behavior as opposed to individual purlin line behavior.

1.3 Scope of Research

The survey of literature indicated that the behavior of roof systems with different restraint conditions is not completely known. To better understand the behavior of typical metal building roof systems, additional data, particularly for multiple purlin line, multiple span systems is needed. This project attempts to fill this gap with the following objectives.

(i) To study the system effect in multi-purlin line systems. System effects on the magnitude of the lateral restraining forces were of particular interest.

(ii) To obtain experimental data to be used to develop analytical models of roof systems.

(iii) To develop fabricating techniques for small scale cold-formed structural members.

(iv) To study the effect of various other parameters on the behavior of roof systems.

To meet these objectives, fabricating and modeling techniques for quarter scale systems were developed and twenty-eight tests were conducted. Results were compared to various analytical models, including those developed by Elhouar [8] in a sister project, which predict the magnitude of lateral restraint forces.

CHAPTER II

DEVELOPMENT OF EXPERIMENTAL PROGRAM

2.1 Prior Use of Models in Structural Engineering Research

Scaled model testing can be traced back to 1922 when Beggs used paper models to obtain mechanical solutions for statically indeterminate structures. Since then models of different types of structures using different materials have been successfully used to develop understanding of the behavior of structures. Simple structural elements like beams, to complex structures like curved bridges and frames, and including hydraulic structures have been modeled. Models have been used to study the effect of both static and dynamic loadings. Reinforced concrete structures are probably modeled more often than steel structures and there are number of papers published in this area, however, they are not considered of interest here. Only three papers on the use of model steel structures were found.

Litle et al [9] reported on the fabrication and testing of one-eighth and one-tenth scale steel wide flange sections, joints and building frames. These scale wide flange sections were fabricated by milling hot rolled bar stock, a reportedly reliable and accurate method of fabricating small scale sections. They tested four milled wide flanged beams, eight fabricated joints, forty-eight

beam-columns and two, two-bay, three-story frames. The frames were one-eighth scale models of a prototype tested at Lehigh University. The authors reported that the results of the small scale model tests can be projected to the prototype structure with reasonable accuracy.

Brennan and Mandel [10] have studied the structural behavior of horizontally curved girder bridges using small scale models. Each component of the curved bridge was modeled and then the components were used to assemble different configurations. They studied the structural action of the horizontally curved steel plate-girder and box-girder bridges of two and three spans. The model did not represent an actual prototype, since their major objective was to show that different configurations of the horizontally curved bridges are possible and that their structural behavior can be successfully studied using small scale models.

Moncarz and Krawinkler [11] modeled structural steel cantilever beams of rectangular cross section. The models were made of CA 510 annealed phosphor bronze material (to represent A36 steel) and were tested under cyclic loading. The ratio of the modulus of elasticity of steel to that of phosphor bronze is 1.92, thus a model to prototype ratio of 1:1.92 was used for all dimensions. They also modeled a single bay, single story frame using phosphor bronze to study its response when subjected to earthquake excitation. They concluded that phosphor bronze is adequate but not an ideal material for models of steel structures subjected to earthquake motion.

To the writer's knowledge, there is no written document on small scale model testing of cold-formed steel

members. However, cold-formed members can probably be modeled more easily and more economically, simply from fabrication considerations, than hot-rolled members.

The general literature on the use of models in research indicates that almost any structure can be modeled provided similitude requirements are satisfied. The effectiveness of the models and the correlation of the results to prototype structures is heavily dependent on the similitude between the model and prototype structures. The model must satisfy some of the similitude requirements which are discussed in the following section.

2.2 Similitude Concepts

The following definitions are from Reference [12]. Two systems are defined to be similar if their corresponding variables are proportional at corresponding locations and times. An example would be a prototype and a model. A prototype is the system of the problem and a model is any system that is similar to it. It is, however, possible to have a model that is not completely similar to its prototype, which are known as dissimilar system.

Models subjected to motion have to satisfy the requirements of geometric, kinematic and kinetic similarity. However, kinematic and kinetic similarity are not a requirement in this study because all loads were applied slow enough to satisfy the static assumption. Two lines or two surfaces are defined to be geometrically similar if the nondimensional functions which specify them in the form $f(X_i) = 0$, where X = nondimensional coordinate, are identical term by term. In other words geometrical similarity requires that

$$(d/x_o)_m = (d/x_o)_p \qquad (2.1)$$

where d_p = a significant length in a prototype p, d_m = a corresponding length in the model m, x_{op} = significant length of the prototype, and x_{om} = significant length of the model corresponding to x_{op}.

Scaling is a technique of relating the prototype and model variables at corresponding points. The scaling factor is defined as the ratio of the corresponding dimensional variables of a prototype and model at corresponding points and is a constant. Therefore, the scaling factor, k_u, is

$$k_u = u(X_i,Y)_p/u(X_i,Y)_m = \text{constant} \qquad (2.2)$$

where $u(X_i,Y)_p$, $u(X_i,Y)_m$ = a significant value of an independent variable 'u' at a specified point on the prototype and model, respectively. When scaling, one of the most important aspects to be considered is size effects. However, with complete similarity, there is no size effect beyond the requirements and results of similarity. Special consideration must be given to possible distortions, if the sizes of the model and the prototype are much different, in which case complete similarity is unlikely. Size effects may or may not be important depending upon the problem.

2.3 Similitude as Applied to the Present Research

A model is defined to be completely similar only when the geometric, kinetic and kinematic similarities, including the similarity in material properties, are

possible. However, one or more of the similarities may not be a requirement for a specific study. For instance, if the load is applied slowly (static test, as in this study), kinetic and kinematic properties are of no consequence. However, material simulation is of significance and may cause difficulty in model studies. In the present study, material manufactured in an identical manner to what is done for prototype material was used. The nominal yield stress of the material was 50 ksi.

The scaling factor, as defined earlier, is the ratio of an independent variable of prototype and model. In the present study, the basic scaling factor k_u is that of length. The other scaling factors are then: (i) area, $1:k_u^2$, (ii) moment of inertia, $1:k_u^4$, (iii) stress 1:1 (because of the material), (iv) tensile load, $1:k_u^2$ and (v) deflection, $1:k_u$.

As an example of geometric similitude requirements, suppose it is required to model the purlin cross section shown in Figure 2.1(a) with a scaling factor of 4.0. Similitude requires all dimensions, flange width (b_f), depth (D), thickness (t), and vertical projection of the edge stiffener (d), radii R_1 through R_4, be divided by the scaling factor 4.0 to obtain the dimensions of the model, Figure 2.1(b). Note that, by the definition of geometrical similarity, the inclination of the edge stiffener with respect to the horizontal for the prototype and the model are same. It follows from similitude that the moment of inertia of the model is 1/256 and the section modulus is 1/64 that of the prototype.

The span of the purlin must also be scaled. A span of 5 ft. was used for all models which corresponds to the

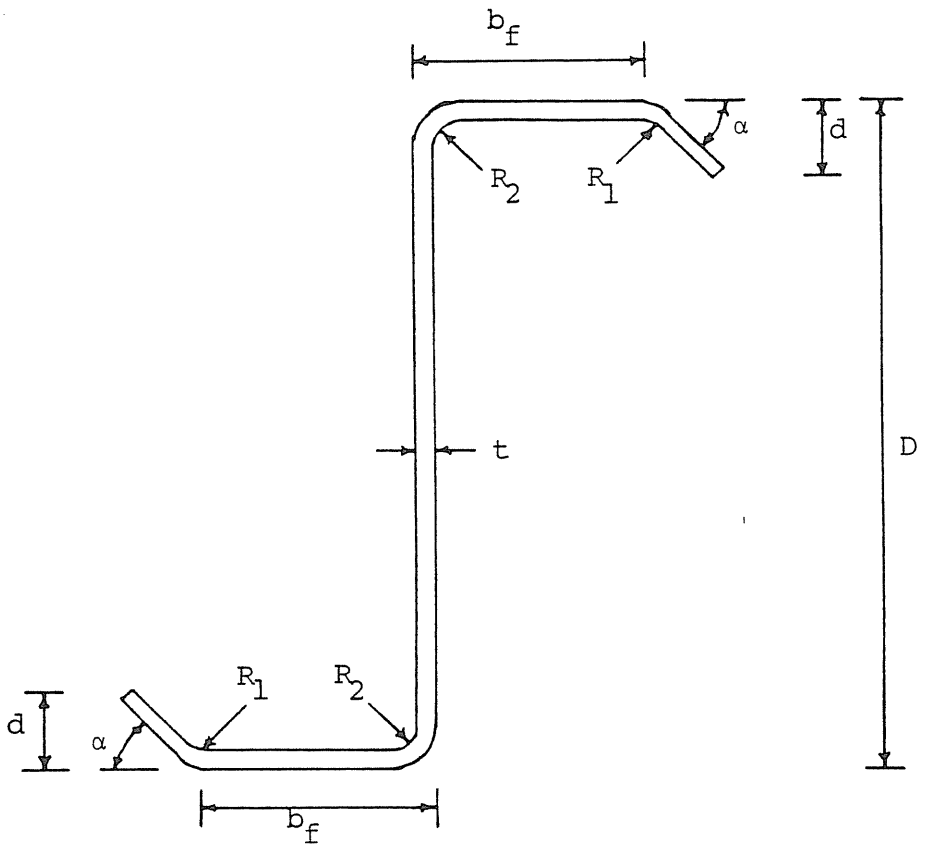

(a) Cross Section Details of Prototype

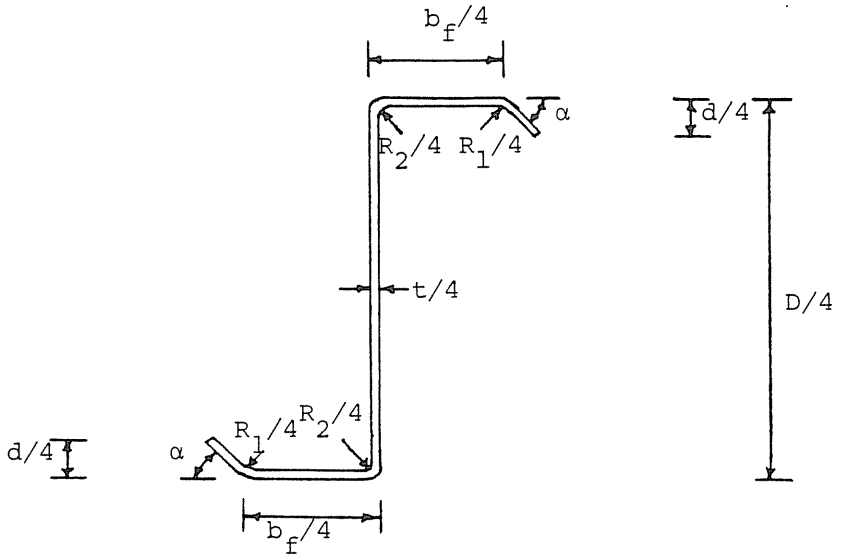

(b) Cross Section Details of Model

Figure 2.1 Z-Purlin Prototype and Model Geometries

prototype span length of 20 ft.

For identical uniform loading on the prototype and model, the corresponding moments in the prototype and model will be in the ratio of 1:16. Thus, the stresses (since the ratio of section modulii is 1:64) will be in the ratio of 1:4 and, for the same material in both prototype and model, it follows that the model will fail at 1/4 of the failure load of the prototype.

It is interesting to note that if a load 'w' per unit length is applied on both the prototype and the model, the midspan deflection of both prototype and model will be same. This is due to the fact that the span length (which must be raised to the fourth power in the deflection calculation) of the model is one-fourth and moment of inertia of the model is 1/256 of the prototype. However, for the given load 'w' per unit length, on both prototype and model, the bending stress in the model is four times that of a corresponding bending stress in the prototype.

2.4 Scope of Experimental Program

The primary purpose of this study was to calibrate the lateral restraining force prediction equations proposed by Elhouar [8]. Secondary objectives were to study the behavior of two purlin line systems with the stiffening edge inclinations of 30^0, 45^0, 60^0, 75^0 and 90^0 with the horizontal and to determine the lateral restraining forces developed at torsional restraints for various roof slopes (0:12, 1/4:12, 1/2:12, 1:12, 1-1/2:12).

The full scale testing of complete system has a number of limitations, cost, effort, safety, etc., thus the models

were used. Fabrication techniques were developed for quarter scale, Z-purlin supported roof systems, and several types of panels and fasteners were evaluated by conducting tests to study the effect of assembly components on the behavior of the system.

All the test results were compared with corresponding predicted values and in some cases with prototype tests. The ultimate capacity of the system was compared with the ultimate capacity of the purlin predicted using AISI criteria for local buckling and the constrained bending assumption. Restraint forces and deflections were compared with Elhouar's analytical model.

CHAPTER III

THE EXPERIMENTAL PROGRAM

3.1 Introduction

This chapter outlines the techniques used to fabricate the quarter scale purlins and describes the test setup, instrumentation and procedures used in the tests. As discussed in the previous chapter, the purpose of the tests was to verify the analytical results obtained in Reference [8] and to determine acceptability of model tests in lieu of prototype tests.

Initial experiments with fabrication and comparison of model test results with full-scale test results showed that quarter scale purlins could be fabricated with reasonable effort and accuracy and that acceptable results could be obtained. Therefore, a scaling factor of 4.0 (quarter scale) was selected for all testing.

Figure 3.1 is photographs of two purlin line, single span and three span roof system test setups. In general, the test setup consisted of two or six purlin lines to which the deck was attached with either machine bolts or self-drilling fasteners. The roof system was supported on simulated rafters and laterally restrained by braces at the rafters (torsional braces), one third points of the span or midspan. The lateral force was measured using calibrated

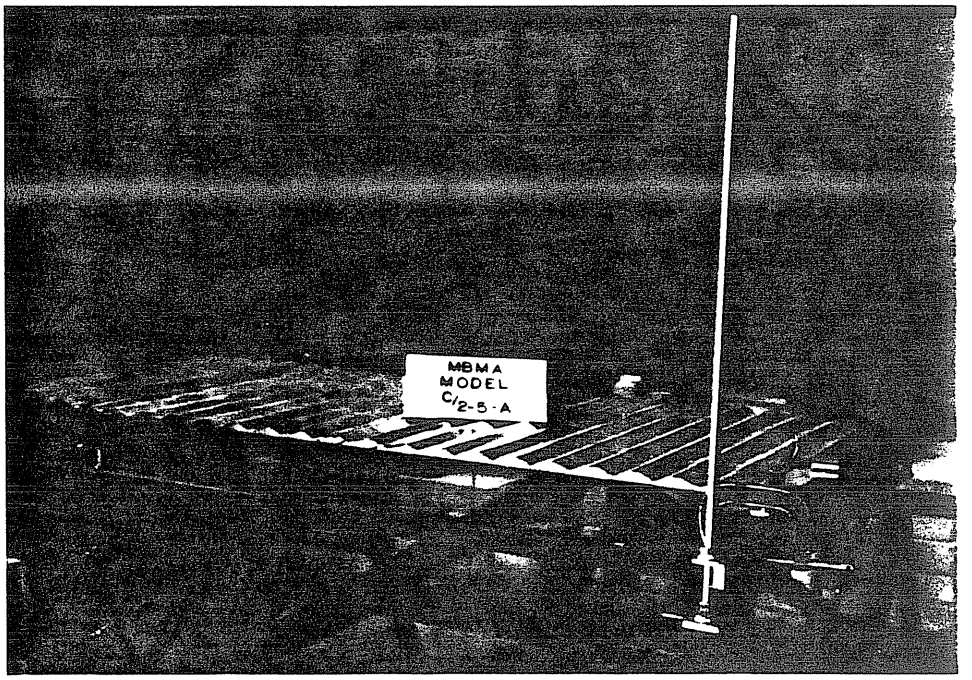

(a) Single Span, Two Purlin Line Test Setup

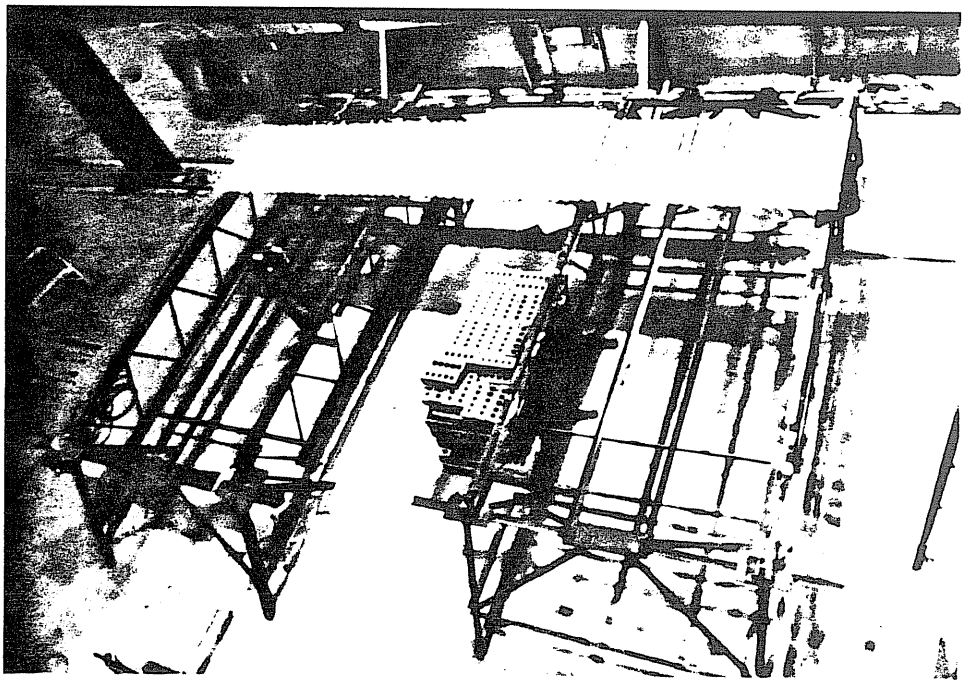

(b) Three Span, Two Purlin Line Test Setup

Figure 3.1 Photographs of the Test Setup

dynamometers. The vertical and lateral displacements of the purlins were measured by transducers. The simulated gravity loading was applied by stacking clay masonry units on the system.

3.2 Test Components

3.2.1 Z-Purlins

The Z-purlins were fabricated at Fears Structural Engineering Laboratory using 24 gage steel sheet material having a nominal yield stress of 50 ksi. The sheet was first sheared to the required width (developed length of the purlin cross-section) and then was bent into a Z-shape without edge stiffeners using a press brake. The edge stiffener was bent to shape by hammering against a mandrel machined from a steel block. The fabrication procedure is shown in Figure 3.2. The press brake could not be used to form the stiffening lips because of its short length. The edge stiffener formed by the mandrel was found to be accurate in length and in orientation.

As discussed in Section 2.2, the similitude requirements for a quarter scale model are that the dimensions of the purlin be reduced by a factor of 4.0. Using this factor, the nominal dimensions of an 8 in. deep 2.5 in. wide purlin are (see Figure 2.1) : D = 2.0 in., d = 0.125 in., b_f = 0.625 in., t = 0.025 in., $R_1 = R_4$ = 0.11 in., $R_2 = R_3$ = 0.0625 in., and $\alpha = 45^0$. The span of the model is also one-fourth the span of the prototype. A span of 5 ft. was used in all tests, representing a full-scale span of 20 ft.

The total depth, flange widths, thickness and the

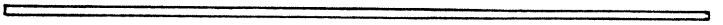

(a) Flat Sheet

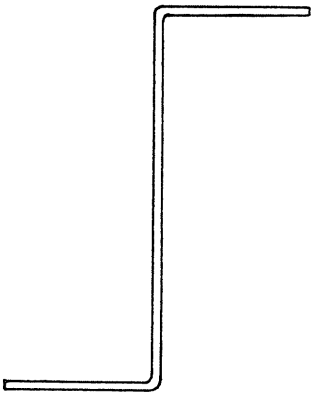

(b) Press Broken Purlin

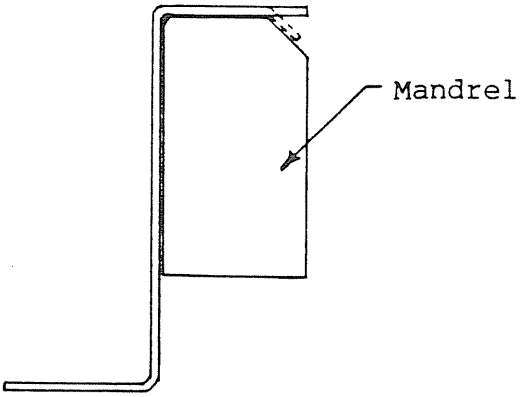

(c) Bending of Edge Stiffener Against Mandrel

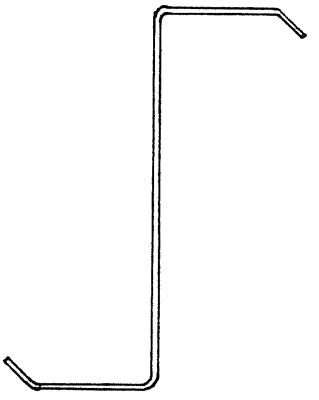

(d) Cold-formed Purlin

Figure 3.2 Fabrication Procedure

vertical projection of the lips were measured after the fabrication of each purlin. The stiffening lip angles were not routinely measured as these will be same as the angle of the mandrels used to form the lips. The radii R_1 thru R_4 were not measured due to the fact that they were quite small and did not significantly affect subsequent analyses. (Nominal radii were used for all analyses).

Standard ASTM tensile test coupons were cut from virgin sheet material and tested. The average measured yield stress from two samples was 51.75 ksi.

The span length for the three span tests was also 5 ft. The two end span purlins were connected by a third intermediate span purlin, overlapping a total length of 7 in.; 3-1/2 in. on either side of the supports. The lap connection used four No. 6-32 machine screws and nuts thru the purlin webs, two on either side of support (see Figure 3.3).

All purlins were analyzed according to the AISI Specifications [1] as discussed in Section 3.3.

3.2.2 Panels and Fasteners

Four types of panels were used in the test program. A corrugated fiber glass panel was used in one test. The system failed due to tearing of the panel at fastener locations and this panel type was discarded. Either corrugated aluminum panels or corrugated steel panels were used in all other tests. Commercially available sheets (2 ft. by 8 ft. or 2 ft. by 10 ft.) were obtained and sheared to the required length, 30 in. for the two purlin system tests and 90 in. for the six purlin system tests. The

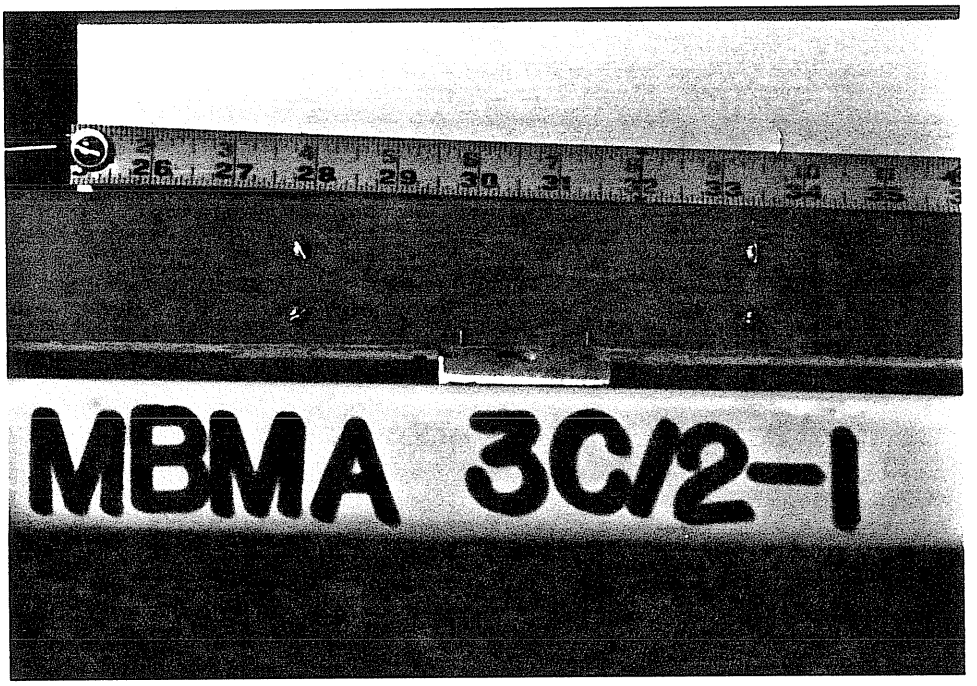

Figure 3.3 Photograph of Lap Connection

cross sectional details of the corrugated metal panels are shown in Figures 3.4 and 3.5.

The panel shear stiffness of the corrugated steel panel was determined by conducting a separate test. Results are reported in Section 3.7.

Two types of fasteners were used to attach panels to the purlin flanges: self-drilling fasteners, No. 6-20 by 1/2 in., and No. 4-40 machine screws and nuts. The panels were fastened to the purlin flange in every corrugation valley, 2.75 in. on center for all types of panels (See Figure 3.5). For multiple purlin tests, the panel to panel connection (sidelap fastening) was made using machine screws spaced at 6 in. on center.

3.3 Analysis of Purlins Using the AISI Specification

The cold-formed purlins were analyzed using the measured dimensions according to the AISI specifications as explained in this section. A computer program written in the "BASIC" code for the Tektronix 4052 minicomputer was used for the analyses. First, the flat-width to thickness ratio of the edge stiffener was determined and compared with 60, the maximum allowable flat-width ratio, to check whether a simple edge stiffener can be used. The maximum allowable compressive stress was then calculated as per Section 3.2 of the AISI Specification [1] depending on the flat-width ratio of the edge stiffener. Based on this maximum allowable stress and according to Section 2.3.1.1 of the Specification, the effective compression flange width was determined. The flange was considered fully effective (b = w), when the flat-width ratio was less than or equal to $171/\sqrt{f}$. Otherwise, the effective width was

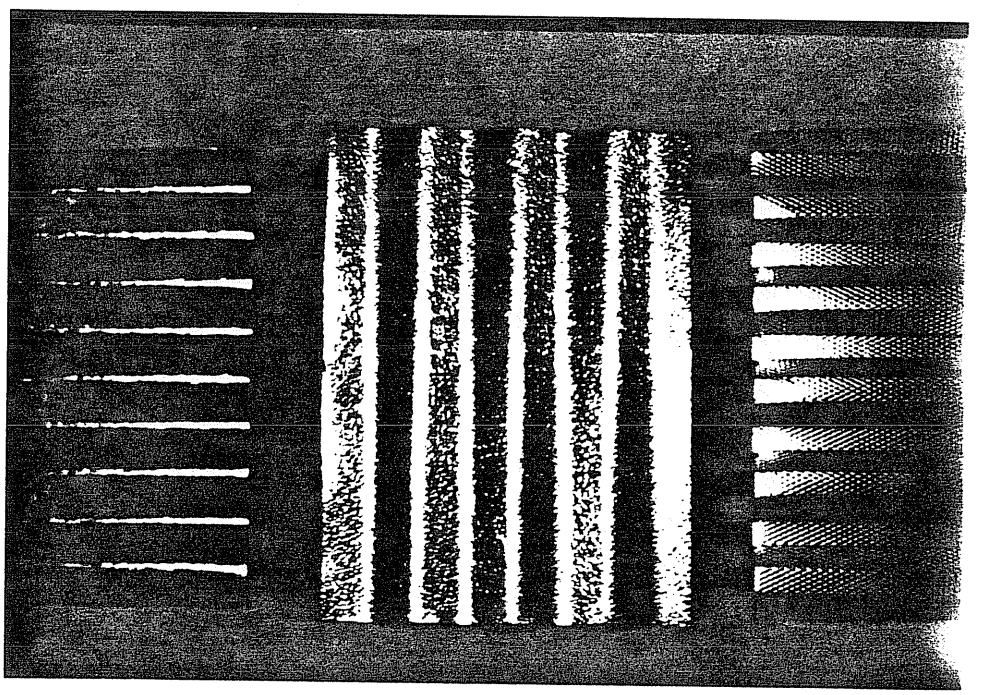

Figure 3.4 Photograph of Panels

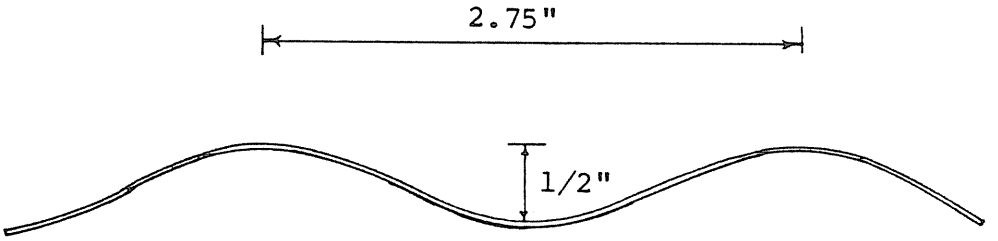

(a) Corrugated Steel Panel

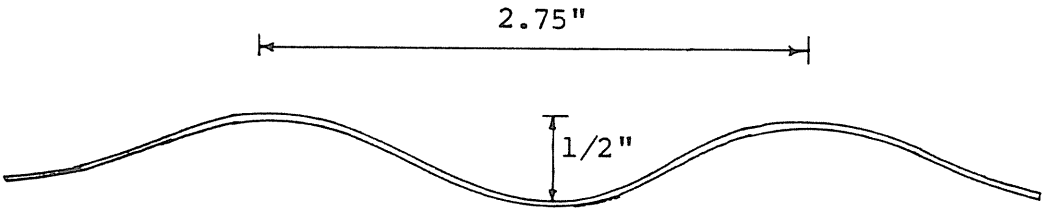

(b) Corrugated Aluminum Panel, Type 1

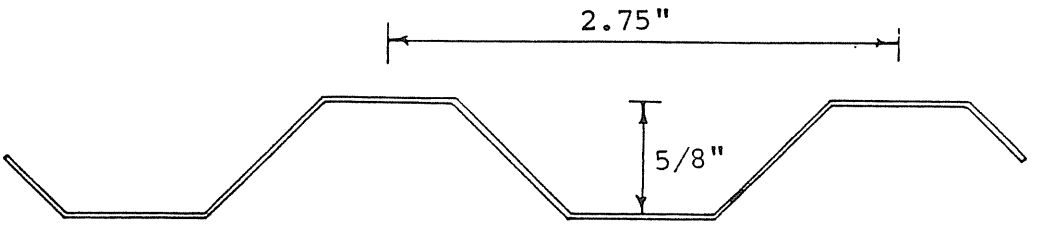

(c) Corrugated Aluminum Panel, Type 2

Figure 3.5 Cross Sectional Details of Panels

determined using Equation 2.3.1-1 of the Specification, i.e.

$$\frac{b}{t} = \frac{253}{\sqrt{f}}\left[1 - \frac{55.3}{(w/t)\sqrt{f}}\right] \qquad (3.1)$$

where b = effective design width, t = thickness, w = flat-width of the flange, f = actual stress in the compression element computed on the basis of the effective design width (equal to the maximum allowable stress for load determination). Finally, the effective section properties were calculated. The failure moment was calculated by multiplying the working moment by 1.67.

For deflection determination, a similar procedure was used. The flanges were considered fully effective (b = w) up to $(w/t)_{lim} = 221/\sqrt{f}$ and AISI Equation 2.3.1-3 was used in lieu of Equation 2.3.1-1.

Also, the moment of inertia of the edge stiffener was calculated and was compared with the minimum moment of inertia of stiffener as given by Equation 2.3.2-1 of the Specification, i.e.

$$I_{min} = 18.3\ t^4 \sqrt{(w/t)^2 - 4{,}000/F_y} \qquad (3.2)$$

but not less than $9.2\ t^4$, where I_{min} = minimum allowable moment of inertia of the stiffener about its own centroidal axis parallel to the stiffened element. This requirement was satisfied in all tests.

3.4 Test Setup

The test setup consisted of structural members

(rafters) spaced at 5 ft. center-to-center and supported by stands which rested on the laboratory floor. The model roof system was supported by the joists. Figure 3.1 shows two photographs of the test setups and the general details are shown in Figure 3.6

Support conditions along a purlin line consisted of one simulated pinned support and the other supports were simulated roller supports. Figure 3.7 shows the details of each support type. The pinned support consisted of a roller between two plates with a groove in each plate. One plate was attached to the bottom flange of the purlin, the second plate was attached to the rafter. The roller support was similar except the plates were flat allowing free movement of the roller.

The torsional and intermediate braces were fabricated from 3/16 in. diameter 12 in. long hydraulic brake line. Each end of the brake line was connected to an universal joint to eliminate rotational restraint at the connection. One of the universal joints was connected to a 3 in. angle welded to a support member. The other universal joint was connected to a 3/16 in. diameter threaded rod which in turn was connected to the purlin. This connection was accomplished by drilling a hole in the purlin web at the proper location and securing the threaded rod in the hole by tightening nuts on either side of the web. For all tests, the braces were placed as near to the top flange as possible, about 1/4 in. down from intersection of the top flange and web.

A slightly different test setup was used for the slope test series. A photograph of this setup is found in Figure 3.8. A 42 in. by 60 in. frame was constructed of

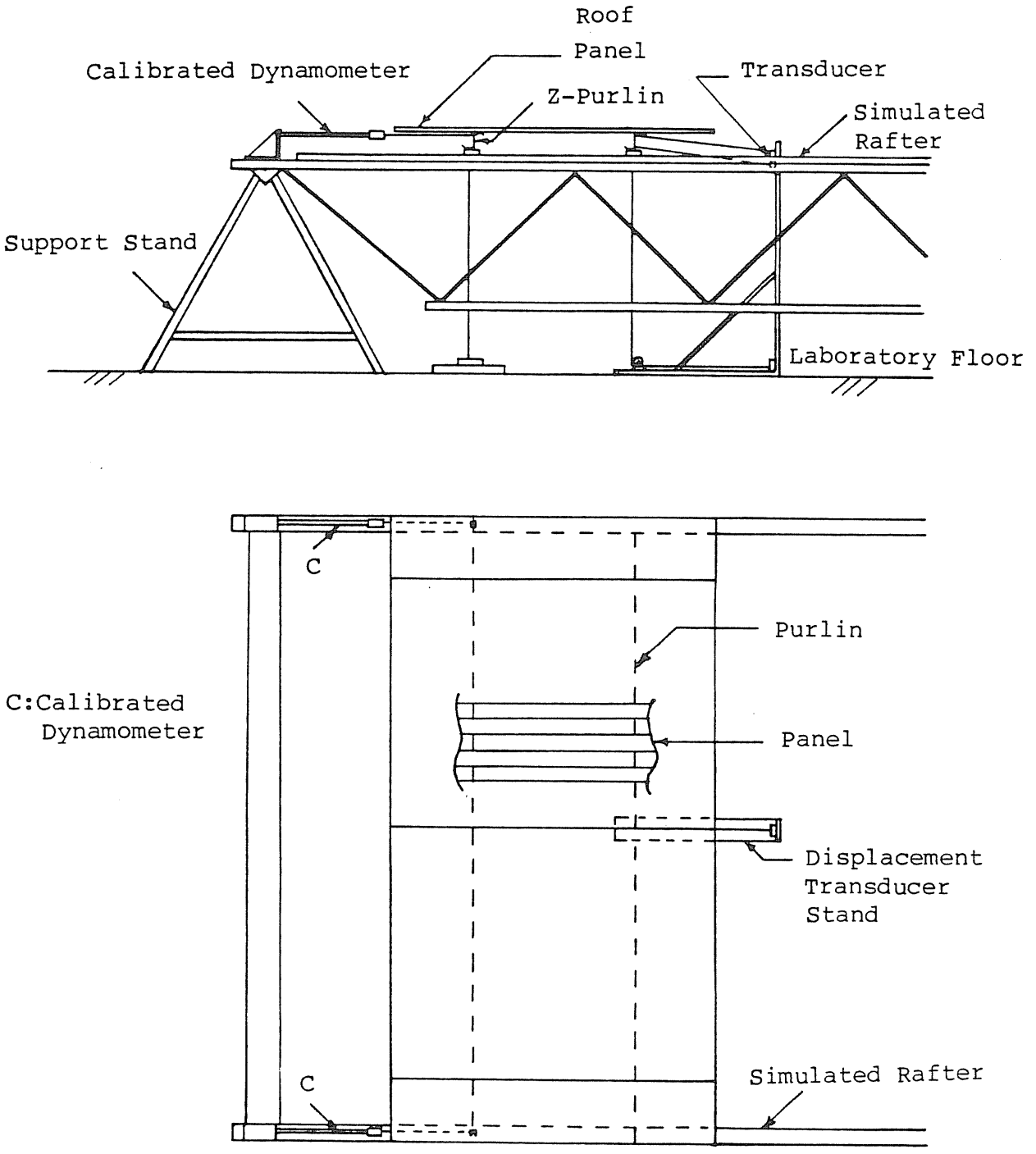

Figure 3.6 Typical Setup Details

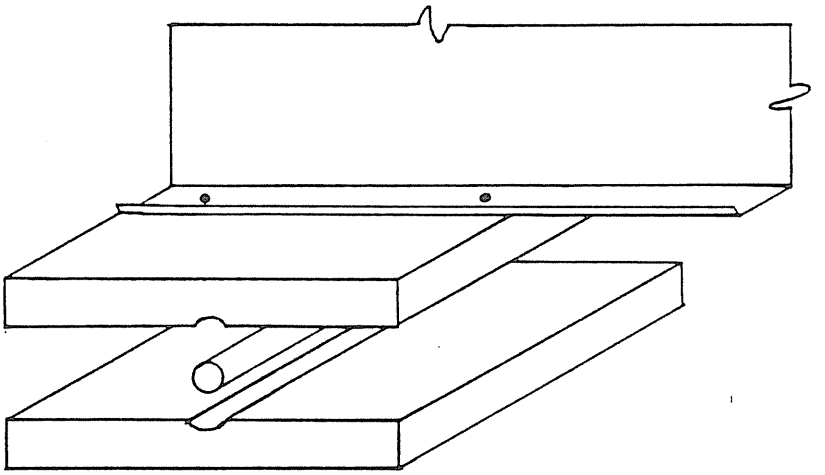

(a) Simulated Hinge Support

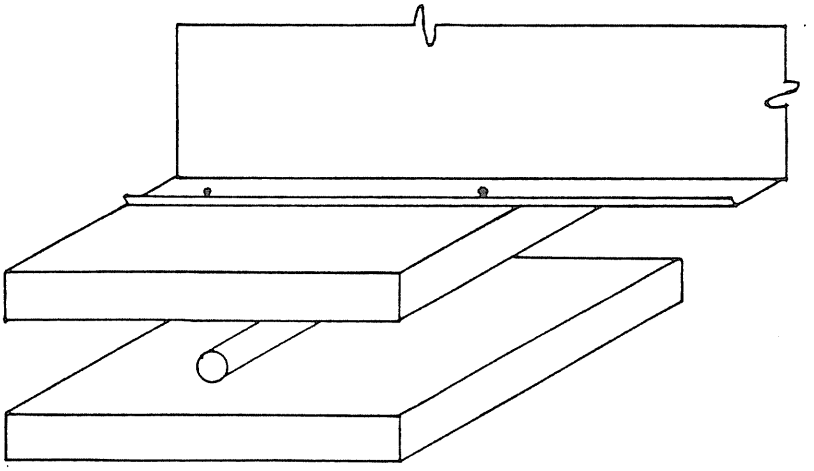

(b) Simulated Roller Support

Figure 3.7 Purlin Support Details

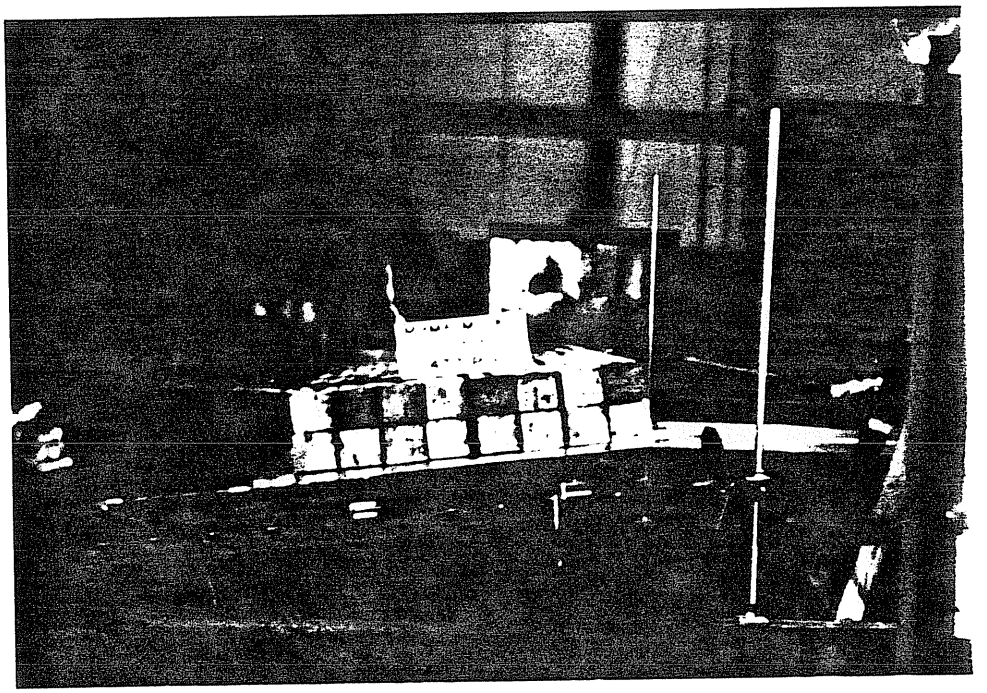

Figure 3.8 Photograph of Roof Slope Test Setup

1-1/2 in. by 1-1/2 in. angles. The 42 in. sides of the frame supported the roof system. One of the long sides of the frame was connected to hinges at the ends. The opposite side was supported by two 5/8 in. diameter threaded rods. Nuts on the rods permitted adjustment of the slope of the frame from 0^0 to 15^0 from the horizontal. Other details were similar to the standard test setup.

For three span tests, two support assemblies separated by 60 in. were used. All other details were same as for the single span test.

3.5 Instrumentation

Instrumentation consisted of calibrated dynamometers to measure lateral restraining forces and linear displacement transducers to measure the vertical deflections and horizontal displacements of the top and bottom purlin flanges.

The calibrated dynamometers were typical intermediate or torsional restraint braces with two strain gages installed at approximately the brace center line. Two electrical resistance strain gages (M-M strain gage type EA-06-050AR-120) were mounted diametrically opposite with the gage length in the longer direction. Prior to testing, the dynamometer was calibrated by gravity loading. Accuracy of the dynamometers was estimated to $\pm$ 1 lb.

Depending upon the test, four to seven linear wire displacement transducers were used to measure vertical and lateral displacements of the purlins. For all single span tests, a transducer was used to measure vertical deflection at the midspan of each purlin. For three span tests,

transducers were used to measure the vertical deflection at the midspan of the end spans along one purlin line.

For most single span tests, four transducers were used to measure the lateral displacements of the tension and compression flange/web intersection of both purlin lines at midspan. For the six purlin line tests, the lateral displacements of the fourth and sixth purlin lines at midspan were measured. For the three span tests, the midspan lateral displacements of one end span of both purlin lines were measured.

Gravity loading was measured by the number of masonry units placed on the test purlins. The average weight of the units was calculated as 4.8 pounds with a standard deviation of 0.1 pounds. The masonry units were uniformly distributed on the roof panel and stacked so as to prevent bridging.

A HP 3497A data acquisition/control unit coupled to a HP 85 desk top computer was used to record, process and print all test data. A HP 7470A two pen plotter was used to plot load versus vertical deflection and the load versus brace force data as the test progressed.

3.6 Testing Procedure

Prior to starting a test, a completed roof assembly was placed in position in the test setup and all instrumentation was connected. At the beginning of each test (except the "slope" series), the system was loaded to approximately 30% of the predicted ultimate load (predicted using AISI local buckling criterion and the constrained bending assumption) to check the test setup and

instrumentation. Following removal of this initial loading, the dynamometers were adjusted so that their measured force was as near as possible to zero.

Next, initial readings of all transducers and dynamometers were recorded. The system was then loaded in approximately 12 plf increments until the predicted working load of the purlins (about 50 plf) was reached. After which the load increment was reduced to approximately 6 plf until 75% to 80% of the predicted ultimate load was reached. The load increment was then further reduced by one-half with loading continuing to failure.

After each load increment, the system was allowed to stand for 2 to 3 minutes before recording data to assure that equilibrium was attained. Output from all transducers and dynamometers were converted from analog to digital signal by the control unit and this signal was reduced and the results printed by the HP 85 computer. Vertical deflection and brace forces were plotted for each load increment as the test progressed. At failure, the failure load, failure mode and other observations were recorded. Photographs were taken during the testing and at failure.

A slightly different procedure was used for slope series tests. In these tests, the roof slope was varied and the system was not loaded to failure. One end of the frame was raised to give the required slope as explained earlier. A load of approximately 24 plf in increments of 6 plf was applied to check the system. This load was then removed and the dynamometers were adjusted so that their measured force was as near as possible to zero force. In this series, the systems were loaded only to the working load (approximately 48 plf). Unloading was done in 12 plf

decrements. Readings were taken at each load level for both the loading and unloading cycles. Upon completion of a test, the support frame was raised without disturbing the system and the next test was conducted.

3.7 Effect of Assembly Components on Test Results

Initially, shear (diaphragm) stiffness of the panels and the type of fasteners used were of concern as to effects on the behavior of the system. The panels and the fasteners could not be accurately scaled because of the availability of material and other limitations. Hence, it was decided to conduct tests with several commercially available panels and fasteners to study the effect of these components on the behavior of the system.

With regard to the panels, analyses of the system with widely varying panel shear stiffness were made by Elhouar [8]. A plot of percent brace force versus panel shear stiffness for a two purlin line system is shown in Figure 3.9. Percent brace force is the total predicted brace force divided by the total applied load expressed as a percent. It can be seen that the change in percent brace force for panel shear stiffness greater than approximately 1500 lb/in is not significant. (A typical metal building thru fastener roof system exhibits a shear stiffness in excess of 2000 lb/in).

This result was also verified by conducting a shear stiffness test and two identical, except for panel type, two purlin line single span tests using two types of panels, corrugated steel panel and corrugated aluminum panel (type 1). The steel panel exhibited a stiffness of approximately 2500 lb/in. By inspection, it was decided

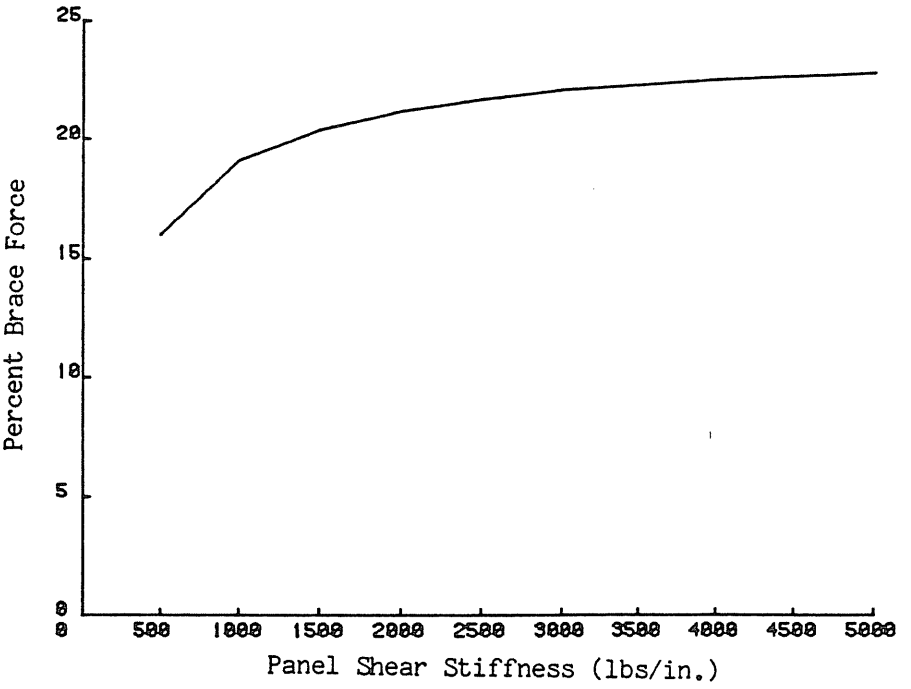

Figure 3.9 Variation of Percent Brace Force with Panel Shear Stiffness

that the stiffness of the aluminum panel was less than that of steel panel. The percent brace force of the system with steel panel system was 19.5% at failure and that of the aluminum panel system was 19.2%. Other results are given in Table 3.1. From these results it was concluded that the shear stiffness of the panels used in the tests did not affect test results.

The effect on the behavior of the system of the fastener type used to attach the panel to the purlin was also studied. Two identical, single span, two purlin line system tests were conducted; one was conducted using 1/2 in. long machine bolts (No. 4-40) and the other using 1/2 in. long self drilling fasteners (No. 6-20). Results of the tests are summarized in Table 3.2. Considering the

Table 3.1

Effect of Panel Shear Stiffness on System Behavior

	Panel Type	
Parameter	Corrugated Steel	Corrugated Aluminum
Test No.	C/2-6-B	C/2-11
Predicted Ultimate Load	84.8 plf.	82.4 plf.
Predicted BF at 100 plf.	105 lbs.	108 lbs.
Failure load	76.5 plf.	71.5 plf.
Failure/Predicted	0.902	0.868
% BF @ working load	18.3%	18.7%
% BF @ Failure load	19.5%	19.2%
Failure Mode	Local Buckling of Compression Lip/Flange	Local Buckling of Compression Lip/flange

Note: BF = Brace Force

Table 3.2

Effect of Fastener on System Behavior

	Fastener Type	
Parameter	Machine Screws	Self Drillers
Test No.	C/2-6-B	C/2-8
Predicted Ultimate Load	84.8 plf.	83.6 plf.
Predicted BF at 100 plf.	105 lbs.	103 lbs.
Failure load	76.5 plf.	79.5 plf.
Failure/Predicted	0.902	0.940
% BF @ Working Load	18.3%	17.9%
% BF @ Failure Load	19.5%	18.3%
Failure Mode	Local Buckling of Compression Lip/Flange	Local Buckling of Compression Lip/Flange

Note: BF = Brace Force

variation in results from tests using cold-formed components, the differences are considered insignificant. Because of easier assembly, machine bolts were used in most tests.

Once the components to be used to fabricate the assemblies were selected a test matrix was formulated to study the parameters explained in earlier chapters.

3.8 Test Matrix

3.8.1 General

A total of seven configurations were selected to study the behavior of roof systems. These tests were grouped into single span and three span tests of two or six purlin lines. Tests of some configurations were conducted more than once to study the variation in test results. The single span tests include the slope and lip angle orientation series as previously discussed.

The complete test matrix, with the parameters for each test, is given in Table 3.3. The nomenclature used to define a test is explained with the following example. Consider Test 3C/2-3, the first digit "3" indicates the number of spans, the letter "C" indicates it is a C-series test. The first digit following the slash, 2 in the example, indicates the number of purlin lines. The last number, 3 in the example, indicates the test number in the particular group. If the digit preceding the letter "C" is missing, it is a single span test.

Table 3.3
Quarter Scale Test Matrix

Test	Number of Purlins	Span(s)		Restraint Configuration			Remarks
		Single	3 Span	Torsional	1/3 Point	Mid-span	
C/2-4	2	X					Purlins in Same Direction
C/2-7	2	X					Purlins in Opposite Direction
C/2-1	2	X		X			
C/2-3-A	2	X		X			
C/2-5-A*	2	X		X			
C/2-6-B	2	X		X			
C/2-8	2	X		X			
C/2-11	2	X		X			
C/2-5-B*	2	X		X			Roof Slope of 1/4:12
C/2-5-C*	2	X		X			Roof Slope of 1/2:12
C/2-5-D*	2	X		X			Roof Slope of 1:12

Table 3.3 (Continued)
Quarter Scale Test Matrix

Test	Number of Purlins	Span(s)		Restraint Configuration			Remarks
		Single	3 Span	Torsional	1/3 Point	Mid-span	
C/2-5-E*	2	X		X			Roof Slope of
C/2-6-A	2	X		X			30^0 Lip Angle
C/2-6-C	2	X		X			60^0 Lip Angle
C/2-6-D	2	X		X			75^0 Lip Angle
C/2-6-E	2	X		X			90^0 Lip Angle
C/2-2	2	X		X			90^0 Lip Angle
C/2-3-B	2	X		X			90^0 Lip Angle
C/2-9@	2	X			X	X	
C/2-10	2	X				X	
C/2-15	2	X			X		
C/6-1	6	X		X			

Table 3.3 (Continued)
Quarter Scale Test Matrix

Test	Number of Purlins	Span(s)		Restraint Configuration			Remarks
		Single	3 Span	Torsional	1/3 Point	Mid-span	
C/6-2	6	X				X	
C/6-3	6	X			X		
3C/2-1	2		X	X			
3C/2-2	2		X	X			
3C/2-3	2		X			X	
3C/2-4	2		X		X		

Notes: 1. All tests were done using 45^0 lip angle purlins and without slope unless noted.

2. The thickness of the purlins are 0.025 in.

* Indicates that purlins were not loaded to failure.

@ Indicates that the lateral restraints were at 1/4 points and not at 1/3 points.

3.8.2 Single Span Tests

A total of twenty-four single span tests were conducted. Of the twenty-four tests, twenty-one were two purlin line systems and three were six purlin line systems. In each subgroup, three configurations were tested:

(i) Torsional restraints at rafters. For the purpose of this study a torsional restraint is defined as restraint which prevents the lateral movement of the Z-purlin top flange, and hence twisting of the Z-purlin, at the rafter locations.

(ii) One third point restraints. Defined as restraint which prevent lateral movement of a point on the purlin web/top flange at the one third points of the span.

(iii) Midspan restraint. Defined as restraint which prevents lateral movement of a point on the purlin web/top flange at the midspan.

Two Purlin Line Systems. Two purlin line systems were studied extensively. All tests were conducted with zero roof slope (flat) and with purlins having edge stiffeners bent at 45^0 from the horizontal, unless noted otherwise. Along with the above three restraint configurations, the following configurations were tested: (a) Two tests were conducted without external restraints; one with purlin flanges facing in the same direction, Test C/2-4, and the second with purlin flanges facing in opposite directions, Test C/2-7. (b) A series of five tests was conducted with restraint configuration (i), but with varying roof slope. The roof slopes considered were 0:12, 1/4:12, 1/2:12, 1:12, 1-1/2:12, Tests C/2-5-A thru C/2-5-E. (c) A series of seven tests with restraint configuration (i) using purlins having lip angles (measured from the horizontal) of 30^0, 45^0, 60^0, 75^0 and 90^0, Tests C/2-6-A thru C/2-6-E, C/2-2

and C/2-3-B. Three tests were conducted using purlins with 90^0 lip angles. (d) One test was conducted with lateral restraints placed at the three quarter points of the span, Test C/2-9. (e) Four tests were conducted with restraint configuration (i), Tests C/2-1, C/2-3-A, C/2-8 and C/2-11. (f) One test was conducted with restraint configuration (ii), Test C/2-12. (g) One test was conducted using restraint configuration (iii), Test C/2-10.

Six Purlin Line Systems. Three six purlin line systems were tested, all purlins had edge stiffeners bent at 45^0 from the horizontal. All the purlins in a test setup were oriented with top flanges facing in the same direction and the roof slope was 0:12. Tests were conducted for each of the three previously described restraint configurations.

In the test with restraint configuration (ii), all six purlin lines were braced near the top flange at one third points of each span, using No. 10-24 threaded rods. For the test with restraint configuration (iii), the purlin lines were similarly braced near the top flange at midspan of each span using No. 10-24 threaded rods. The lines of rods were connected to an external restraint using a calibrated dynamometer.

3.8.3 Three Span Tests

Four tests in this series were conducted; all tests used two purlin lines. Two tests were conducted with restraint configuration (i) and one test each with restraint configurations (ii) and (iii). The same restraint system was used in each span.

All twenty-eight tests were conducted in accordance

with the procedures outlined in Section 3.6. The results obtained from the above tests are analyzed in the following chapter.

CHAPTER IV

ANALYSIS OF EXPERIMENTAL RESULTS

4.1 Comparison with Prototype Tests

The success of a model study is largely dependent on how well results compare with results from prototype tests. Hence, it is appropriate at this point to compare results of several model tests with available prototype test results. These comparisons are made in the following paragraphs.

One of the most important comparisons is the purlin material properties of the prototype and model. The material for purlin models were obtained from a manufacturer of prototype purlins and panels. The chemical and mechanical properties of the two materials were similar. The typical stress-strain relationship of the purlin materials are given in Figure 4.1. The stress-strain relationship of the model material was found to be similar to that of prototype material. The measured yield stress of the model material (51.75 ksi, from coupon tests) was less than the average measured yield stress of the prototype material (57.9 ksi).

In the previous chapter, it was shown that the fasteners and the panels used did not affect the behavior of the model roof system. With similar purlin material

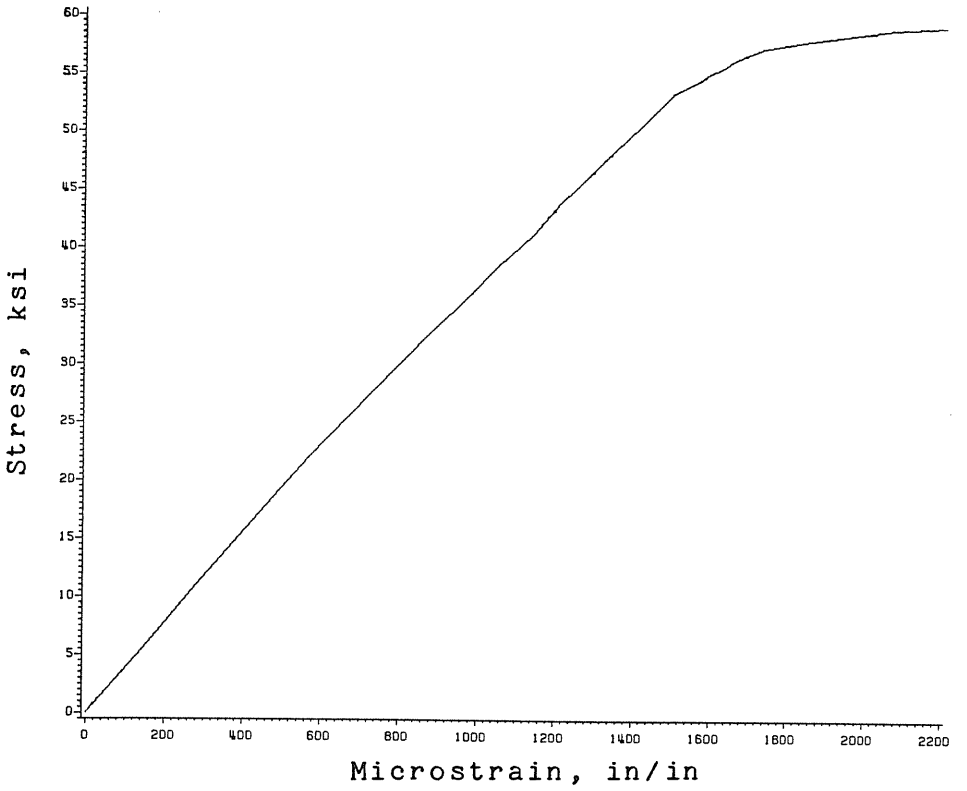

Figure 4.1 Typical Stress-Strain Relationship of Purlin Materials

properties, it is left to compare the behavior of prototype and model roof systems. For comparison purposes, both model and prototype results are expressed in nondimensional numbers. Hence, the load on the system, measured vertical deflection and measured lateral restraining forces of model and prototype were divided by the predicted ultimate load, predicted vertical deflection at failure and predicted lateral restraining force at failure.

Figure 4.2 shows normalized load versus normalized vertical deflection of model Tests C/2-6-B, C/2-8 and C/2-11 and prototype Tests III and VI from Reference [3]. Configuration (i), torsional restraints at the rafters, was

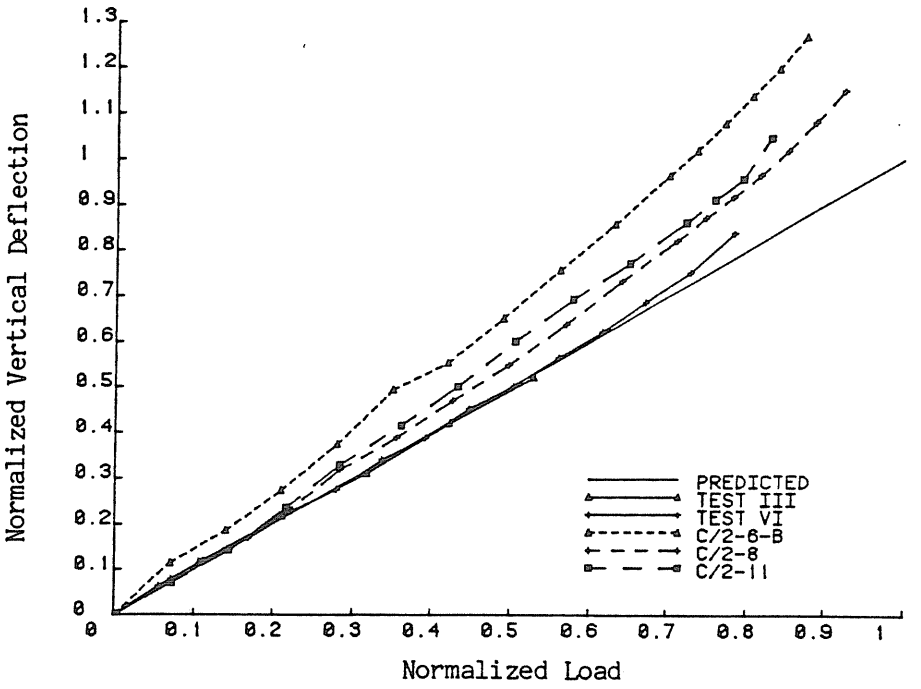

Figure 4.2 Comparison of Prototype and Model Vertical Deflections

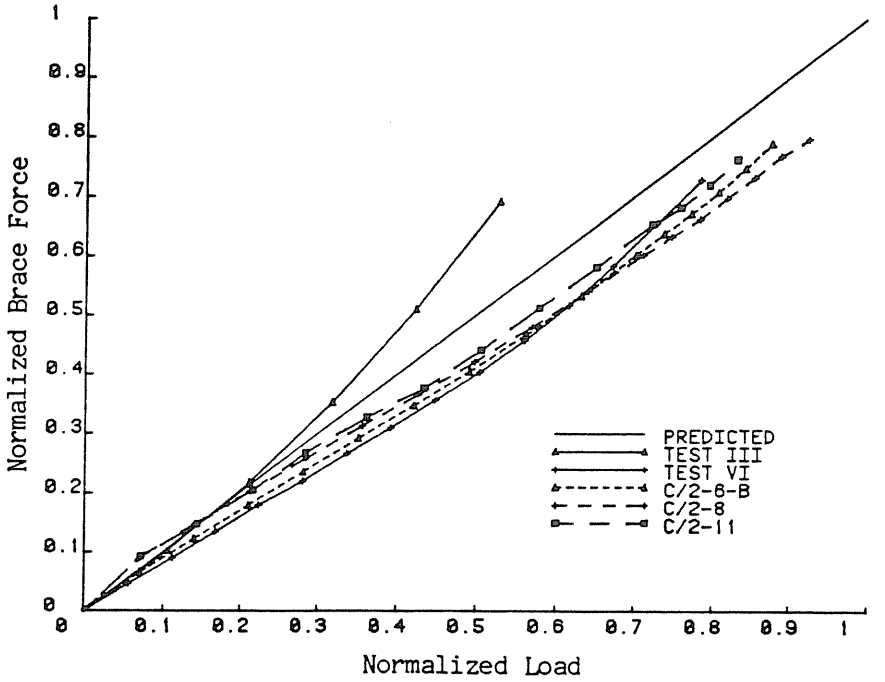

Figure 4.3 Comparison of Prototype and Model Brace Forces

used in all tests. Similarly, a plot of normalized load versus normalized lateral restraining force for the same tests are shown in Figure 4.3. Also shown in the figures are predicted deflection and predicted lateral brace forces.

It is evident from Figures 4.2 and 4.3 that overall system behavior of the models is similar to the prototype. Generally, however, the normalized vertical deflections from the model tests were greater than those from the corresponding prototype tests. In some cases, the model deflections were over 30% greater than the predicted deflections. The normalized brace forces for both the model and prototype tests, Figure 4.3, were somewhat less (about 10%) than the predicted brace forces with one exception, prototype Test III. Otherwise, the normalized brace forces of prototype Test VI and model Tests C/2-6-B, C/2-8 and C/2-11 were found to be in excellent agreement. Similar results were obtained for comparisons between results of Tests 3C/2-2 and 3A/2-2, conducted at Fears Structural Engineering Laboratory (unpublished).

Having shown good agreement between the model and prototype roof system with configuration (i), it is generalized that, good agreement will exist between models and prototype structures for other configurations as well.

4.2 Analytical and Experimental Comparisons

4.2.1 Basis of Comparisons

In the previous chapter, it was mentioned that vertical deflections, lateral deflections and lateral

restraining forces were measured and recorded, as well as, ultimate load and failure mode. These experimental results are now compared to deflection predictions using standard strength of material formulae, to failure loads calculated using AISI local buckling criteria and the constrained bending assumption and to results from the analytical procedure developed by Elhouar [8].

4.2.2 Vertical Deflections

Midspan vertical deflections of the single span, two purlin line systems were predicted considering the purlin to be simply supported, constrained to deflect in a vertical plane and carrying uniform loading. The midspan vertical deflections are given by

$$\Delta = 5\ wL^4/384\ EI \qquad (4.1)$$

where I = the moment of inertia of the purlin with respect to the horizontal axis, w = uniform load, L = span, and E = modulus of elasticity.

For all other tests, the midspan deflections were calculated using a stiffness analysis program developed by Elhouar [8]. The single span, two purlin line systems were also analyzed using Elhouar's program. Midspan deflections obtained by the program and those given by Equation 4.1 were not significantly different.

Theoretical lateral deflections were also obtained by the same computer program. These deflections were compared to deflection measured at the compression flange/web junction during the tests.

4.2.3 Ultimate Loads

Predicted ultimate load was calculated using AISI local buckling provisions with the constrained bending assumption. Effective width provisions were used for the flange element and reduced allowable stresses, depending on slenderness, for the edge stiffener and web. Edge stiffener adequacy was checked and all radii considered. The calculated working load was then multiplied by 1.67 to obtain the predicted cross-section moment capacity from which ultimate span loading was calculated.

4.2.4 Lateral Restraint Forces

As mentioned in the earlier chapters, the main purpose of this study was to compare the measured lateral restraint forces to predicted forces from the analytical model proposed by Elhouar [8]. In this analytical model, the roof system is considered to be made up of space frame and space truss components. The purlins are considered as space frame members and the panels modeled using space truss members. The lateral restraints are considered to be space truss members. The complete space truss/space frame structure is analyzed using a stiffness analysis program. The force in the lateral restraint members is the predicted lateral restraint force.

For the series of tests in which the roof slope was varied, Tests C/2-5-A thru E, the analytical value of the lateral restraining force was obtained by subtracting a factor from the lateral restraining force of the system at zero roof slope. The factor is

$$\tan \theta \times w_g \qquad (4.2)$$

where Θ = roof slope and w_g = total gravity load on the system.

In the following sections, the analytical values obtained as above are compared to corresponding experimental values from the various tests. The comparisons are generally in the form of graphs.

In the following discussion, "first purlin" or "purlin #1" means the eavemost purlin or the purlin to which the lateral restraints are attached. Similarly, the "second purlin" or "purlin #2" indicates the purlin next to "purlin #1" towards the ridgemost purlin, and so forth to the "ridge" purlin.

4.3 Lip Angle Orientation Test Series

The purpose of this series was to study the effect of lip angle on the ultimate strength of the system. Five tests were conducted with configuration (i), torsional restraints. In all the tests, the vertical deflections were greater than theoretical by 2% to 12%. The vertical deflections of the first purlin were greater than the second purlin by 3% to 5%.

The ratios of the experimental ultimate loads W_u to the predicted ultimate loads W_p are shown in Table 4.1. As expected, the ratio increased from 78.1% for the 30^0 lip angle test to 97.5% for the 75^0 lip angle test. For the three 90^0 lip angle tests, the results were 92.2%, 86.9% and 90.2%.

A plot of W_u/W_p versus lip angle is found in Figure

4.4. The solid line is a prediction equation developed from prototype tests [13]:

$$R = 0.62 + 0.00523\alpha \qquad (4.3)$$

where R = reduction due to lip angle inclination and α = lip angle measured from the horizontal, in degrees. Solving for α with R = 1.0, gives $\alpha = 72.65^0$. Hence, the system is expected to develop full capacity if the lip angle is greater than 72.65^0.

For all tests, except the tests using the 90^0 edge stiffener inclination, the measured restraint force was less than predicted as seen from Table 4.1. For the 90^0 tests, the measured and predicted forces were nearly identical.

The failure mode for all tests was local buckling of compression lip/flange near midspan.

4.4 Roof Slope Test Series

The purpose of this series of tests was to study the effect of roof slope on the lateral restraining forces. Five tests using configuration (i) were made. The same system was used for each test as the assemblies were not loaded to failure. Tests were conducted at slopes of 0:12 1/4:12, 1/2:12, 1:12, 1-1/2:12 and loaded to working load (approximately 48 plf).

For all tests, the vertical deflections of both purlins were greater by 20% to 30% than the predicted values. The vertical deflections of purlin #1 were greater than the purlin #2 by about 3% to 5%.

Table 4.1

Summary of Results for Lip Angle Test Series

Lip angle	W_p plf	W_u plf	W_u/W_p	% Brace force at Working Load		% Brace force at Failure	
				Predicted	Measured	Predicted	Measured
30°	87.70	68.53	78.1	22.60	20.9	22.60	21.2
45°	84.83	76.50	90.3	21.70	18.3	21.70	19.5
60°	86.67	82.43	95.1	22.00	18.1	22.00	18.4
75°	85.54	83.43	97.5	21.30	17.6	21.30	17.2
90°	84.01	77.5	92.2	20.10	20.1	20.10	21.1
90°	82.26	71.5	86.9	20.27	28.6	20.27	31.0
90°	84.83	76.5	90.2	21.72	18.3	21.72	19.5

W_p = Predicted Ultimate Load

W_u = Failure Load

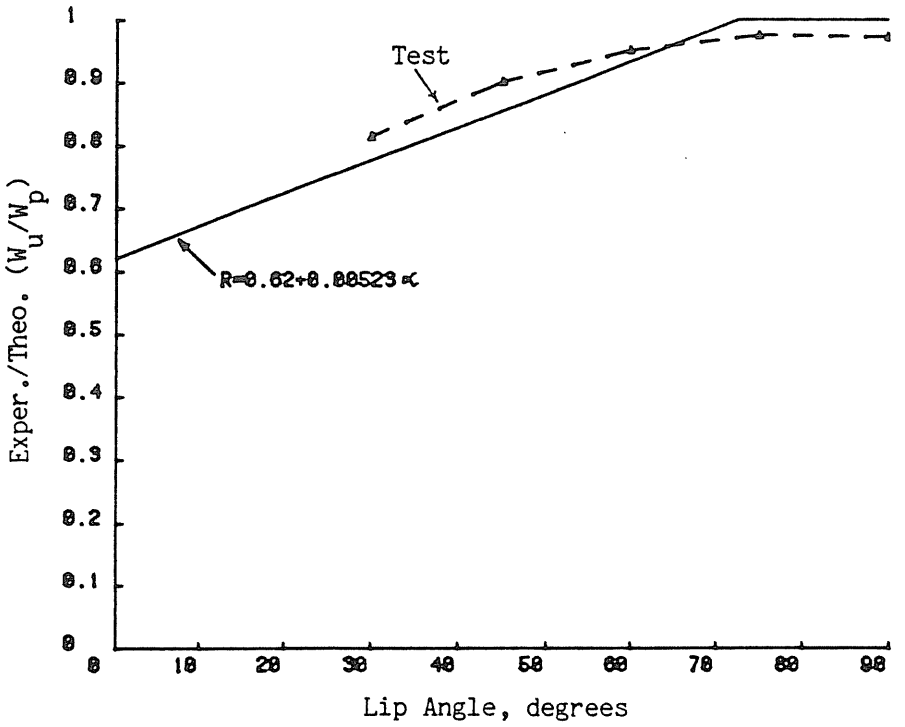

Figure 4.4 Strength Ratio versus Lip Angle

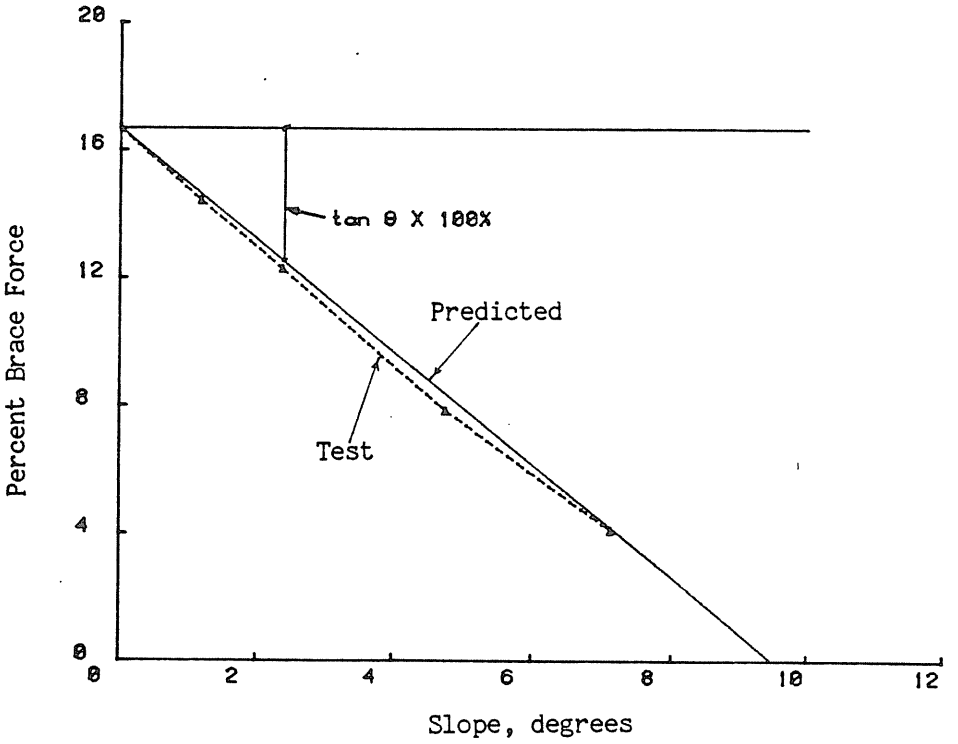

Figure 4.5 Percent Brace force versus Roof Slope

A plot of percent brace force versus roof slope in degrees is shown in Figure 4.5. Equation 4.2 was used to determine the theoretical line in this figure. The percent brace force measured for the zero roof slope test was used as the initial point. It can be seen from Figure 4.5 that the predicted and measured behavior are very similar. Thus, for any system having a roof slope, the required restraint force can be predicted from the restraint force requirement for a system with zero roof slope and subtracting the factor from Equation 4.2.

4.5 Single Span Tests

The purpose of these tests was to study the behavior of roof systems with different configurations. Both two and six purlin line systems were tested with configurations

(i), (ii), and (iii). Two additional configurations were tested using no external restraint.

4.5.1 Two Purlin Line Systems

No Lateral Restraints. Two tests were conducted to determine the ultimate strength of the system when no lateral restraints are provided. In one test, both purlin flanges were facing in the opposite direction, Test C/2-7, in the other test the purlin flanges were facing in the same direction, Test C/2-4. Both systems were constructed with purlins having edge stiffeners inclined at 45^0 from the horizontal. The systems were loaded to failure.

For both tests, the measured vertical deflections were greater than the predicted vertical deflections by 15% to 40% as shown in Figure 4.6. The vertical deflections of test C/2-4 were greater than the vertical deflections of test C/2-7 at same load, Figure 4.6.

The predicted ultimate strength, failure load and failure mode for both systems are given in Table 4.2. The failure load for the system with purlin flanges facing in the same direction was approximately 50% of the predicted strength and that for the opposed purlin system, approximately 90%.

The failure modes for the two tests were different. The failure mode for Test C/2-4 was excessive lateral deflection. Test C/2-7 failed by local buckling of the compression lip/flange.

Torsional restraints. These tests are considered as base tests. The purpose was to measure lateral restraint

Table 4.2

Summary of Test Results for Single Span, Two Purlin Line Systems with No Lateral Restraints

Test	Parameter	Failure Load plf W_u	Predicted Load plf W_p	W_u/W_p	Failure Mode
C/2-4	Purlins in same Direction	41.7	84.2	49.5%	Excessive Lateral Deflection
C/2-7	Purlins in opposite direction	77.5	86.7	89.3%	Local Buckling of Compression Lip/Flange

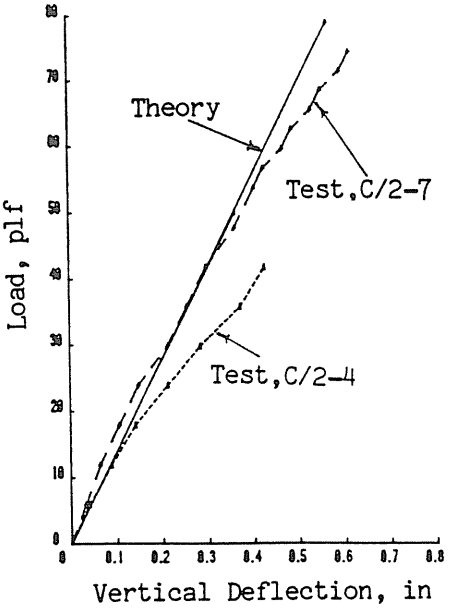

Figure 4.6 Load versus Deflection, No Restraints

forces developed in the torsional restraints, configuration (i), using purlins with edge stiffeners oriented at 45^0 from the horizontal. All tests were loaded to failure and conducted at zero roof slope.

The measured vertical deflections were greater than the predicted vertical deflections in all the tests. The general behavior was as shown in Figure 4.7. In all tests, the vertical deflections of the second purlin were greater than the vertical deflection of first purlin by about 3% to 5%.

In all tests, the initial portion of the load versus lateral restraint force curve has a "kink", Figure 4.8, which is attributed to difficulties in positioning the lateral restraints so that no prestress existed prior to the beginning of the test. The lateral restraining forces as a percent of total load near working load and at failure are given in Table 4.3. The lateral restraining forces at working load varied from 17.9% to 24.6% of the total vertical load for the five tests. The percent lateral force generally increased slightly with increasing vertical load on the system. The percent lateral forces at failure ranged from 18.3% to 25.6%. The predicted restraint forces varied from 20.3% to 21.7% of the applied vertical loads.

Also given in Table 4.3 are the ultimate strengths of the five two purlin line systems. The ultimate strength varied from 75% to 95% of the predicted constrained bending strength. From Table 4.3, it can be seen that there is a definite relationship between the ultimate strength and the lateral restraining force developed. The higher the brace force, the smaller the ratio of W_u to W_p and vice versa.

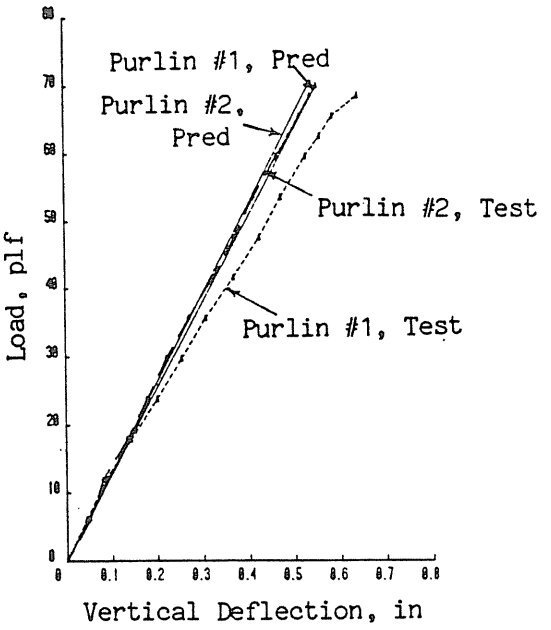

Figure 4.7 Typical Load versus Vertical Deflection Plot

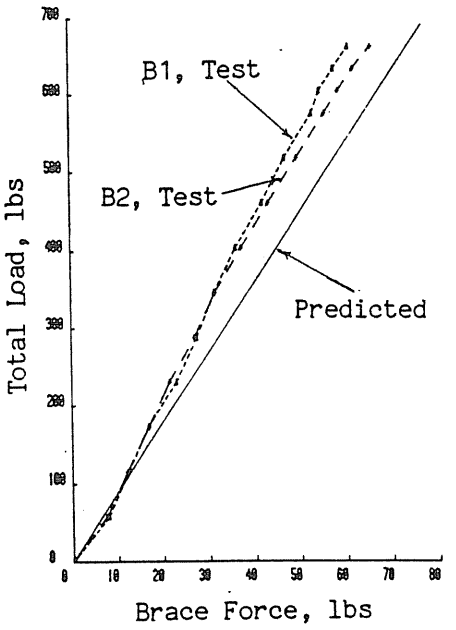

Figure 4.8 Typical Load versus Brace Force Plot

Table 4.3
Summary of Test Results for Single Span, Two Purlin Line Systems with Torsional Restraints

Test	% Brace Force @ Working Load	% Brace Force @ Failure	Predicted % Brace Force	Failure Load W_u plf	Predicted Ultimate Load W_p plf	W_u/W_p %
C/2-1	24.4	25.1	21.4	70.5	83.9	84.0
C/2-3-A	24.6	25.6	20.3	65.5	86.9	75.4
C/2-6-B	18.3	19.5	21.7	76.5	84.8	90.2
C/2-8	17.9	18.3	21.3	79.4	83.6	95.0
C/2-11	18.7	19.2	20.9	71.5	82.3	86.9

The mode of failure for all the above tests was local buckling of the compression lip/flange near midspan. In some cases both purlins failed while in some only the laterally restrained purlin failed. The failure mode for all tests was similar to the failure mode of the prototype purlins. Figure 4.9 shows the photograph of compression flange/lip local buckling for a model test.

One-Third Point Restraints. The purpose of this test was to determine the forces developed in lateral restraints located at the third points of the span and to compare results with the predicted restraining forces. For this test, restraint configuration (ii) was used with 45^0 edge stiffener purlins. The system used a zero roof slope and was loaded to failure. The actual failure load was 76.5 plf; whereas, the constrained bending predicted load was 82.6 plf.

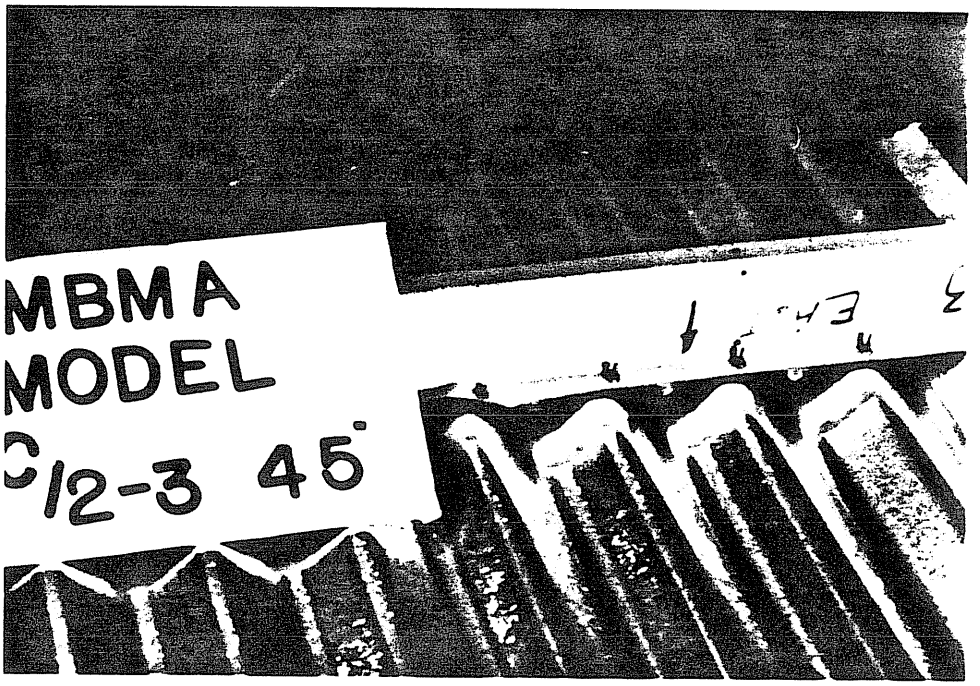

Figure 4.9 Photograph of Failure Mode

The measured lateral restraining forces were less than the predicted lateral forces as shown in Figure 4.10. The predicted total restraint force was 21.2% of total vertical load.

The system failed at 92.6% of the predicted ultimate load. The failure mode was local buckling of compression lip/flange near midspan of both purlins.

Mid-Span Restraint. The purpose of this test was to determine the lateral force developed in a system with configuration (iii). The test was conducted at zero roof slope, with 45^0 edge stiffener and the system was loaded to failure. The failure load was 70.5 plf and the predicted failure load was 85.3 plf.

The measured lateral restraining force were less than

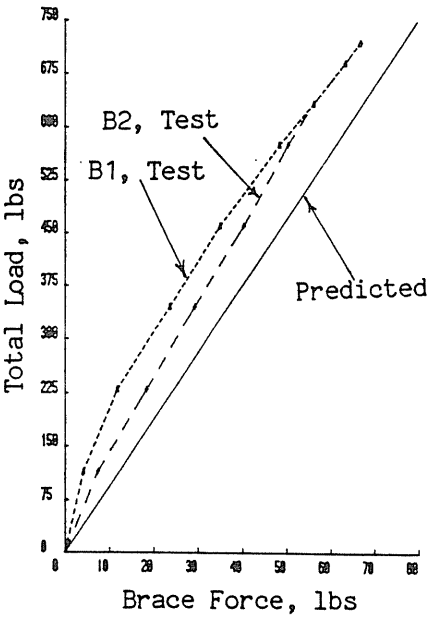

Figure 4.10 Load versus Brace Force, One-Third Point Restraints

the predicted force as shown in Figure 4.11. The predicted restraint force was 18.6%.

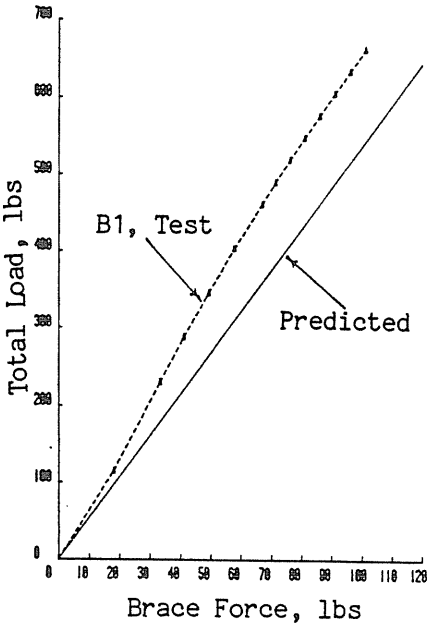

Figure 4.11 Load versus Brace Force, Midspan Restraint

The system developed 82.7% of the predicted strength. The failure mode was local buckling of the compression lip/flange of both purlins near midspan.

Quarter Points Restraints. In this test, lateral restraints were provided at the three quarter points along the span. Test parameters were zero roof slope and 45^0 edge stiffeners. The system was loaded to failure. The failure load was 74.5 plf and the predicted failure load was 83.1 plf.

The lateral restraining force was 19.3% of total load at working load and 20.1% at failure load. The predicted restraint force was 22.9% of vertical load. Figure 4.12

shows the restraint force versus applied load relationship.

The system developed 89.7% of the predicted failure load. The failure occurred near midspan of the first purlin due to the local buckling of compression lip/flange.

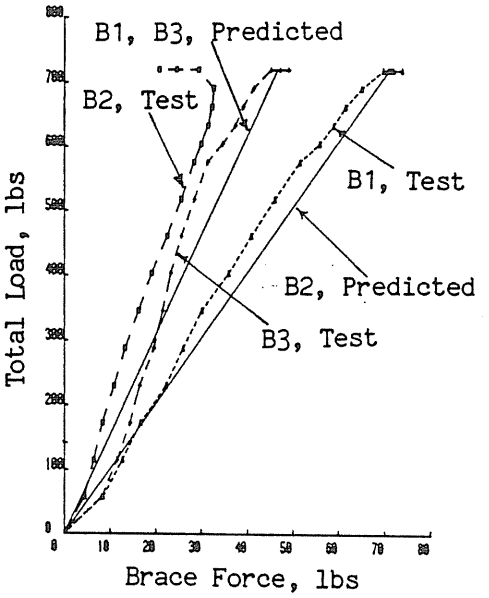

Figure 4.12 Load versus Brace Force, Quarter Point Restraints

4.5.2 Six Purlin Line Systems

Torsional Restraints. Only one test was conducted with this configuration. The purpose was to study the accumulation of lateral restraining force in a multiple purlin line system. The system was loaded to failure.

This setup was slightly different from the other two six purlin line systems. The roof deck did not extend beyond the flanges of the exterior purlins and thus only one-half of the load applied to an intermediate purlin was

applied to an exterior purlin.

The deflections of fourth and sixth purlin were measured. The measured deflections were greater than the predicted deflections, by nearly 75% for the sixth purlin. This was caused by bridging action of the panel, since the intermediate purlins were more heavily loaded, deflected more and allowed the panel to span between outside purlins.

The measured lateral restraining forces were nearly equal to the predicted lateral force, as shown in Figure 4.13. The percent lateral restraining force at about working load was 18.2% and at failure, 20.3%. The predicted value was 17.5%.

The failure load was 88.2 plf and the predicted

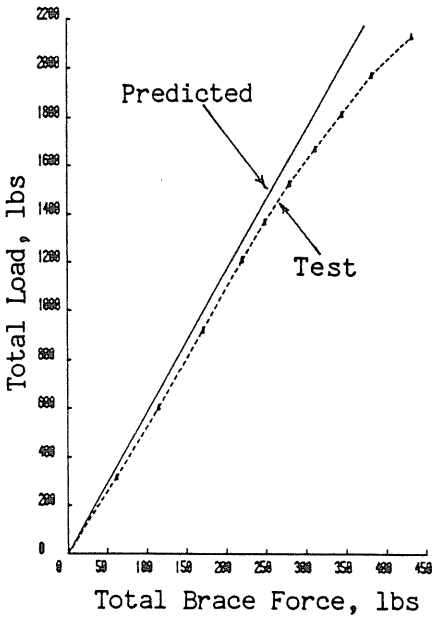

Figure 4.13 Load versus Brace Force, Six Purlin Line, Torsional Restraints

failure load was 86.4 plf. This is the only test where the predicted failure load is less than the actual failure load. The probable cause is panel bridging action which would tend to decrease the load on the intermediate purlins, that is, the actual load on the intermediate purlins would be less than that calculated directly from tributary area. The failure mode was local buckling of the compression lip/flange of all purlins.

One-Third Point Restraints. The purpose of this test was to determine the lateral restraining force developed in a six purlin line system with a one-third point lateral restraint system. All purlins were loaded equally as the roof panels extended beyond the flanges of the outside purlins. The experimental failure load was 78.7 plf and the predicted failure load was 81.8 plf.

The measured vertical deflections of the fourth and sixth purlins were greater, by 10% to 35%, than predicted deflections. The vertical deflections of fourth purlin were greater than that of sixth purlin by about 3% to 5%. The lateral deflections of a purlin tension flange were not measured. The lateral deflections of the compression flange of the sixth purlin were greater than that of the fourth purlin. Both compression flanges were in the direction of the "ridge" purlin. The lateral deflections of the sixth purlin was about 150% greater than those of the fourth purlin at first increment of load; at failure they were about 40% greater.

The measured lateral restraining forces were less than the predicted lateral forces, Figure 4.14. The lateral forces increased almost linearly with the increase in vertical load. The percent lateral restraining force at

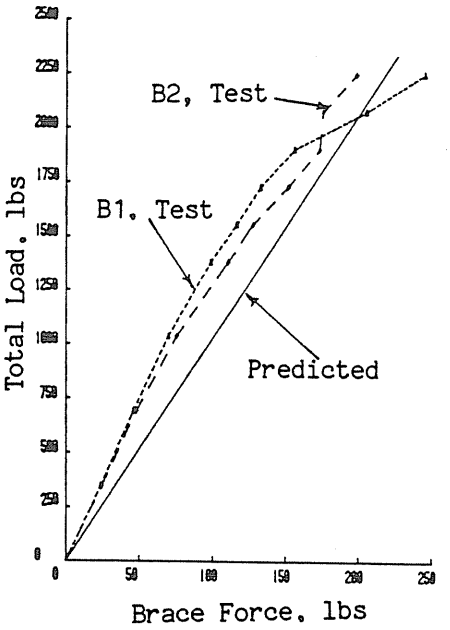

Figure 4.14 Load versus Brace Force, Six Purlin Line, One-Third Point Restraints

working load was 15.7% of total vertical load and at failure, 19.8% of total vertical load. The predicted value was 19.5%.

Failure of the system occurred at 96.2% of the predicted failure load. The failure mode was local buckling of the compression lip/flange near the one-third point of the span. However, before total failure, local buckling of the compression lip/flange of the first purlin near one of the lateral restraint was observed (71.5 plf).

Mid-Span Restraint. The purpose of this test was similar to that of a two purlin system with configuration (iii). The failure of the system occurred at 59.6 plf and the predicted failure load was 83.2 plf. The webs of the

first two purlins were reinforced near the lateral restraint on either side by a 0.025 in. thick, 3 in. wide plate to prevent premature buckling of the web due to the concentrated forces from the restraint member.

The vertical deflections of the fourth and sixth purlins were greater than the predicted deflections, by 20% to 40%. The vertical deflections of the sixth purlin were greater than those of the vertical deflections of the fourth purlin by about 3% to 5%. The lateral deflections of purlin compression flanges were not measured. The tension flange lateral deflections of the sixth purlin were greater than those of the fourth purlin. Both purlins moved in the direction of the ridge. The lateral deflection of the sixth purlin was about 90% greater than that of the fourth purlin at the first load increment and was about 22% greater than that of the fourth purlin at failure.

The measured lateral restraining force was less than the predicted lateral force, see Figure 4.15. The restraining force increased almost linearly with increase in gravity loading. At working load, the restraining force was 14.5% of the total gravity load and at failure it was 15.4%. The predicted value was 16.4%.

Local buckling of the compression lip/flange of the first purlin near midspan was noticed at 53.6 plf. On a slight increase in loading, the compression lip/flange of the second and third purlins buckled locally and then the entire system collapsed at 71.6% of the predicted failure load.

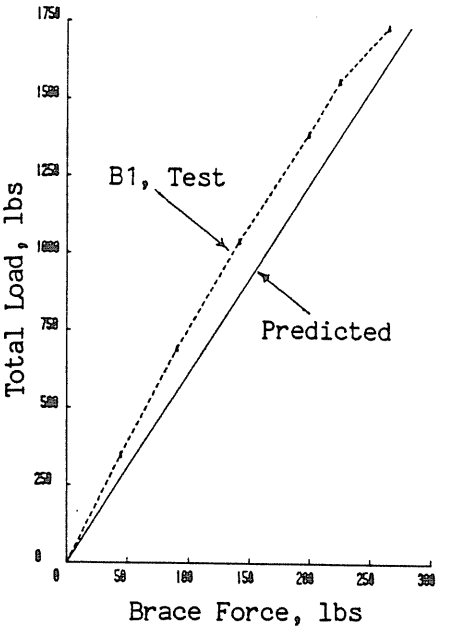

Figure 4.15 Load versus Brace Force, Six Purlin Line, Midspan Restraint

4.6 Three Span Tests

In this series, four tests were conducted using configurations (i), (ii) and (iii). Only two purlin line systems were tested. All tests used purlins with 45^0 edge stiffener orientations, were conducted at zero roof slope and were loaded to failure.

Torsional restraints. These systems, Tests 3C/2-1 and 3C/2-2, were laterally restrained at each rafter. In the following discussion, the restraints at the extreme supports (rafters) are referred to as exterior lateral restraints and are denoted by "B1" and "B4". The restraints at the intermediate supports are referred to as the interior lateral restraints and are denoted by "B2" and "B3". The actual failure loads were 148 plf for Test

3C/2-1 and 100.4 plf for Test 3C/2-2. For both tests and the predicted failure load was 135.5 plf.

For both tests, the vertical deflections of the end span were greater than the predicted vertical deflections by about 20%. The end span vertical deflections of the first purlin were greater than the second purlin by about 3% to 5%. The intermediate span vertical deflections were greater than the predicted deflections by about 200%, however, the actual deflections are very small, less than 0.25 in. The purlins deflected laterally in the ridge direction.

The measured lateral restraining forces for Test 3C/2-2 were greater than the predicted lateral forces as shown in Figure 4.16. At working load (83.4 plf), the total lateral force was 24.7% of the total vertical load. At the same load, the sum of exterior lateral restraining forces was 8.1% of the total load, and the sum of interior lateral forces was 16.6% of the total load. The corresponding predicted values are 18.5%, 6.4% and 12.1%, respectively. At 95.3 plf, the total lateral restraining force was 26.1% of total vertical load. The sum of the exterior lateral forces was 8.1% and the sum of interior lateral forces was 18.0%. The predicted values are the same. It is clear from the above results that the exterior lateral force increased linearly with increase in gravity loading and the interior lateral force increased in an increasing manner with increase in gravity loading.

The ultimate strength of the system was 74.1% of the predicted strength. The failure mode was local buckling of the compression lip/flange of the first purlin on the end span, near the midspan.

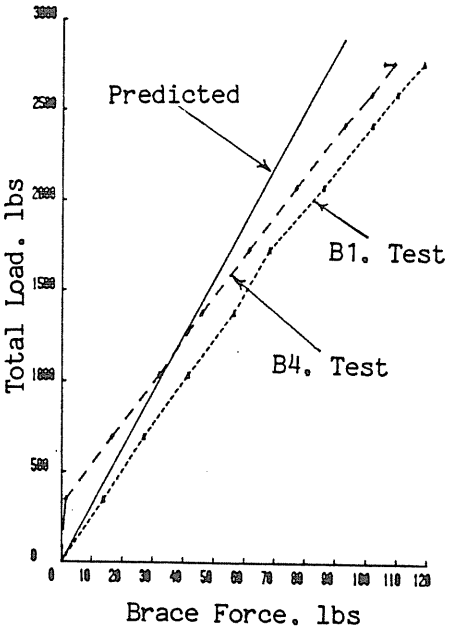

(a) Brace Forces at External Rafters

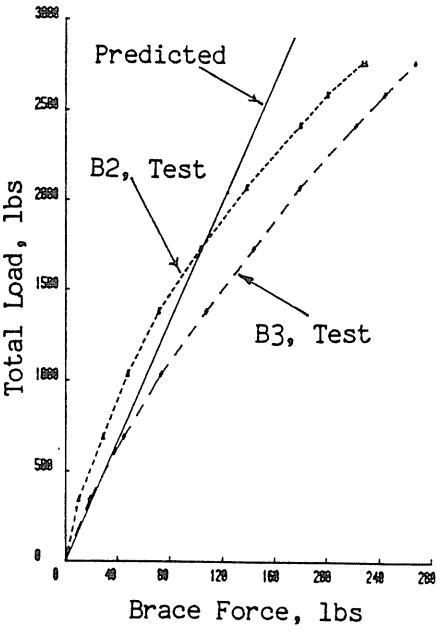

(b) Brace Forces at Internal Rafters

Figure 4.16 Load versus Brace Force, Three Span, Torsional Restraints

One-Third Point Restraints. Test 3C/2-4 was similar to the single span Test C/2-12 with configuration (ii), that is, lateral restraints were placed at the one-third points of each span. The failure load was 107.5 plf and the predicted failure load was 136 plf.

All measured vertical deflections were greater than the predicted vertical deflections. The end span deflections were 20% to 30% greater than predicted. The vertical deflections of the intermediate span were about 300% greater than predicted. Again, the magnitudes are very small. The purlins deflected laterally in the ridge direction.

In the following discussion, "B1" thru "B6" corresponds to the lateral restraints from one end of the system to the other end respectively. Only four lateral restraining forces "B1", "B2", "B4", and "B6" were measured. "B3" was assumed to be same as "B4" and "B5" was assumed to be same as "B2" because of symmetry. At working load, 83.4 plf, the total lateral force was 17.2% of total vertical load. Out of which, the sum of the end span lateral forces was 12.3% of total load and the interior span lateral forces, 4.9% of total load. The predicted values were 19.1%, 13.0% and 6.1%, respectively. At failure, 107.5 plf, the total lateral restraining force was 21.2% of the total load. The sum of the end span lateral forces was 13.6% of total load and the interior span lateral forces was 7.6% of total load. The lateral forces increased in an increasing manner with the increase in gravity load, Figure 4.17.

The system failed at 79.0% of the predicted failure load due to local buckling of the compression lip/flange in

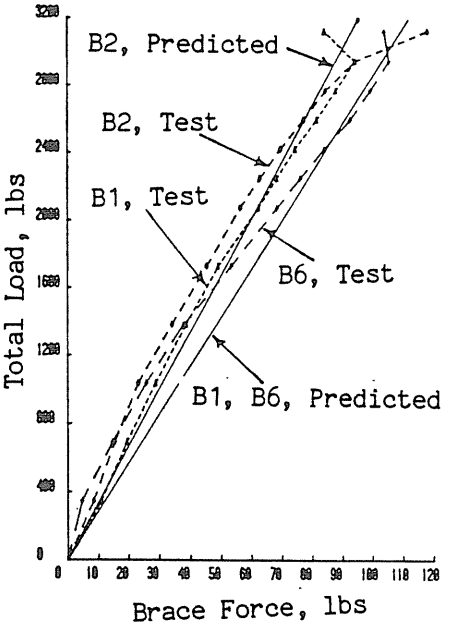

(a) Brace Forces in External Spans

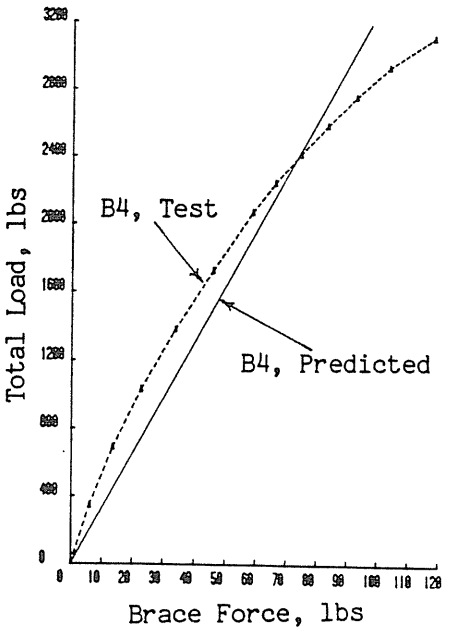

(b) Brace Force in Internal Span

Figure 4.17 Load versus Brace Force, Three Span, One-Third Point Restraints

the end span of the first purlin line near the outer one-third point.

Mid-Span Restraint. This test, Test 3C/2-3 was similar to the single span Test C/2-10, with configuration (iii). Lateral restraints were placed at the midspan of each span. The failure load was 95.3 plf and the predicted failure load was 135 plf.

The vertical deflections in each end span were greater than the predicted deflections. The end span vertical deflections of the first purlin were greater than the second purlin by 3% to 5%. The vertical deflections of the intermediate span were greater than the predicted deflections by more than 300%, again very small magnitudes are involved. The purlins deflected laterally in the ridge direction.

The lateral restraining forces increased in an increasing manner with the increase in vertical load, Figure 4.18. The sum of the measured lateral forces in the end spans was less than the predicted lateral force up to the working load, 83.4 plf. The measured intermediate span lateral force was greater than the predicted lateral force. At working load, the total brace force was 19% of the total vertical load. The sum of the end span lateral restraining forces was 11.5% of the total load and the intermediate span restraint force was 7.5% of the total load. Corresponding predicted values are 16.8%, 11.5% and 5.3%. At failure, the total lateral force was 21.4% of the total vertical load. The sum of the end span lateral forces at failure was 13.0% of the total load and the intermediate span lateral force was 8.4% of the total load.

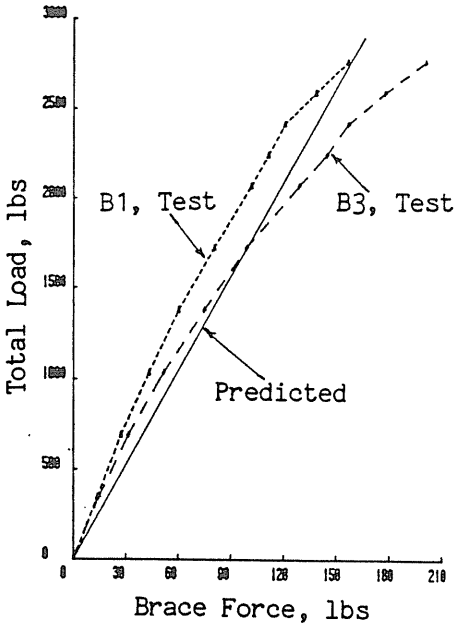

(a) Brace Forces in External Spans

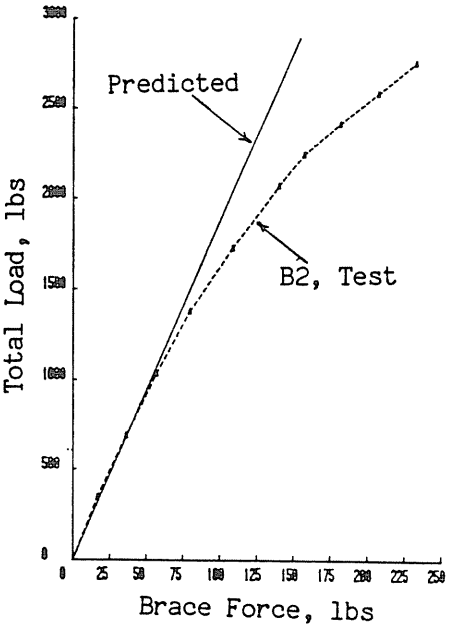

(b) Brace Force in Internal Span

Figure 4.18 Load versus Brace Force, Three Span Midspan Restraint

Failure occurred at 70.6% of the predicted failure load. The failure mode was local buckling of the compression lip/flange of the first purlin near midspan of all three spans.

4.7 Comparisons of Single Span Tests with Three Span Tests

In this section, the single, span two purlin line system test results are compared with corresponding three span, two purlin line system test results. The results are compared using plots of normalized load versus normalized total brace force. To normalize, the load or brace force is divided by the predicted failure load or predicted brace force at failure load.

Torsional Restraints. Figure 4.19 shows normalized brace force versus normalized load for single span tests

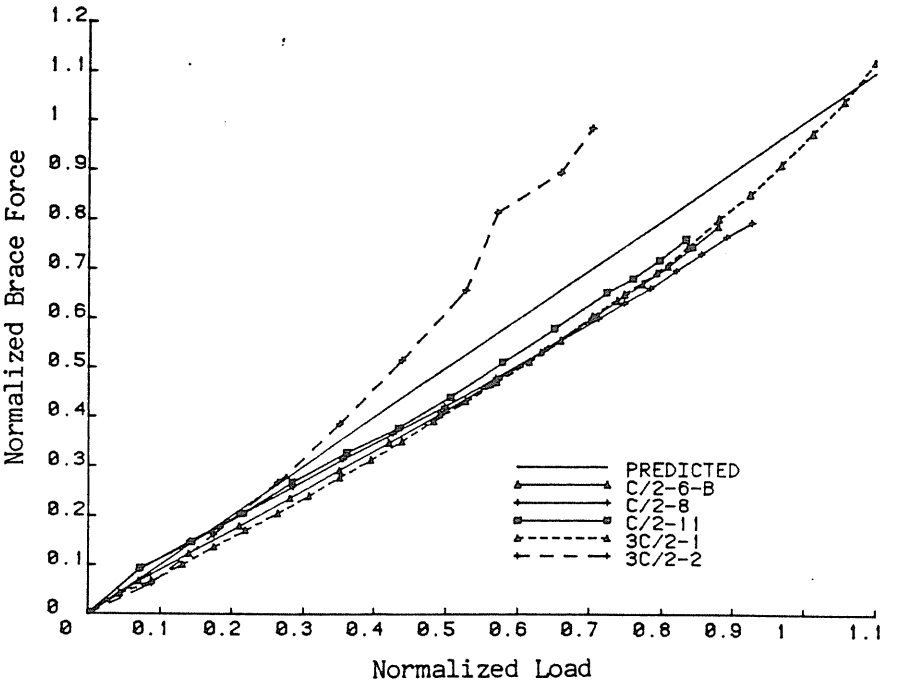

Figure 4.19 Comparison of Single Span and Three Span, Torsional Restraints

and three span tests conducted with torsional restraints, configuration (i). Except for Test 3C/2-2, all measured brace forces are slightly less than the predicted brace forces and the normalized brace force for the single span and three span tests are almost equal.

One-Third Point Restraints. A plot of normalized brace force versus normalized load for single span and three span tests with one-third point restraints, configuration (ii), is found in Figure 4.20. Generally, the measured brace force was less than the predicted brace force. For a given normalized load, the normalized brace force in a three span test was greater than the single span test. That is, percent brace force (as a percent of total vertical load) in a three span test was greater than the percent brace force in a single span test. The brace forces increased in an increasing manner with additional

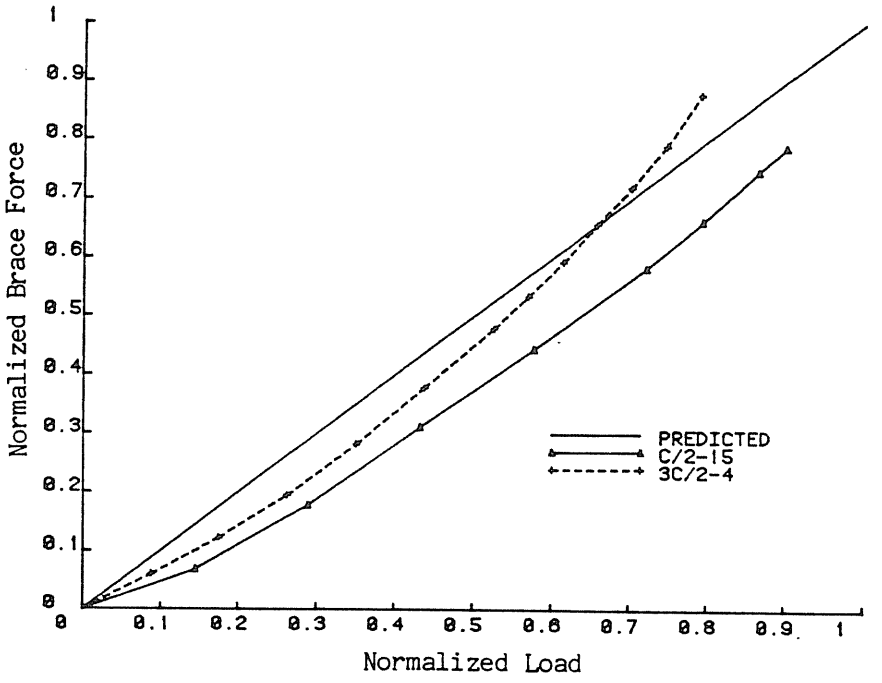

Figure 4.20 Comparison of Single Span and Three Span, One-Third Point Restraints

applied load. For a three span test, the total brace force was conservative up to about 66% of the predicted failure load.

Midspan Restraint. Figure 4.21 shows a plot of normalized brace force versus normalized load for single span and three span tests with midspan restraint. The behavior of the systems were similar to systems with one-third point restraints (See Figure 4.20). The percent brace force in the three span test was greater than the percent brace force in the single span test. The total brace force in the three span system was conservative up to 43.8% of the predicted failure load.

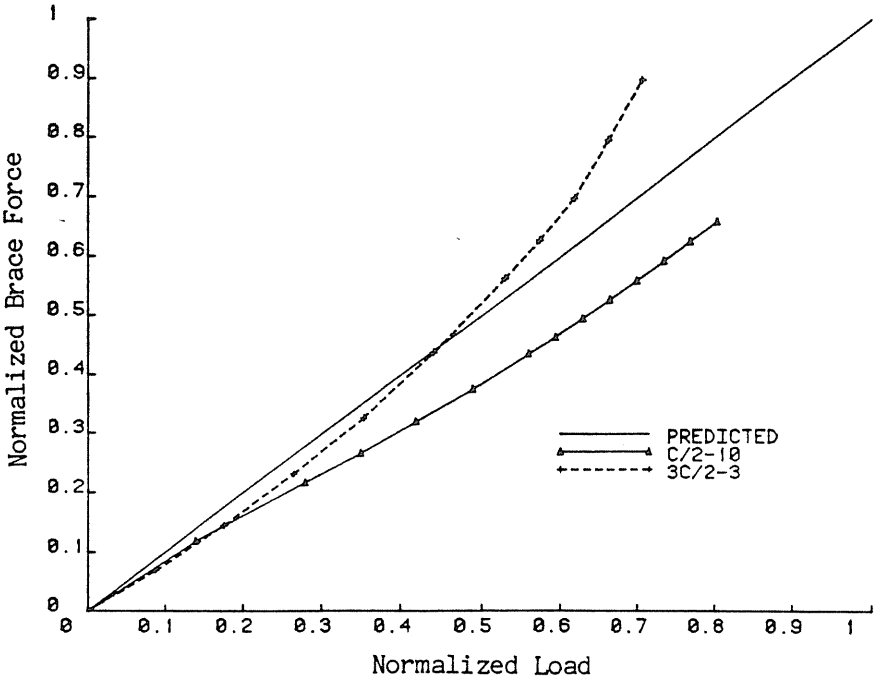

Figure 4.21 Comparison of Single Span and Three Span, Midspan Restraint

CHAPTER V

SUMMARY AND FINDINGS

5.1 Summary

An experimental investigation involving 28 quarter-scale model tests of different configurations and parameters was described in the preceding chapters. The purpose of the test program was to determine restraint requirements and other data for complete, thru fastener, Z-purlin supported roof systems subjected to gravity loading. The data acquired was used to develop an analytical model in a sister project by Elhouar [8]. Fabrication techniques for small scale cold-formed structural members were developed as a necessary part of the study.

The test roof systems were analytically modeled as a space frame space truss structures using Elhouar's stiffness analysis techniques. These results, as well as other analytical and prototype results, were compared with the model tests results. In general, test results compared well with both predictions and prototype test results.

5.2 Findings

The results of this study show that cold-formed structural members can be effectively studied using quarter

scale models. Similar prototype and model test results were found to compare well; failure modes for both sets were similar. Evaluation of costs, effort, loading mechanisms, test setups and other variables shows that model based research is a desirable alternative to full scale testing

The measured vertical deflections in the model tests were always greater than predicted deflections based on the constrained bending assumption. Midspan vertical deflections generally exceeded predicted deflections by 10% to 20%. Similar results have also been reported for prototype tests.

The analytical model proposed by Elhouar [8] was found to adequately predict the lateral restraining forces for all of the configurations tested. The predictions are generally conservative; the maximum being 15%. Unconservative predictions did not exceed 10%.

It was found that no separate equations or procedures are required to predict restraint forces in systems with roof slope. The restraint forces for a system with roof slope can be found using the restraint force for the same system with zero roof slope and then correcting for roof slope by subtracting the component of the applied load parallel to the plane of the roof.

The effect of edge stiffener orientation on restraint force was found to be insignificant when all other purlin dimensions are the same.

Tests using restraints at the one third points resulted in the least restraint forces, measured as a

percent of total applied load. The percent restraint force developed for configurations using third point restraints were found to be 12% to 25% less than those for identical torsional restraint configurations. The magnitude of restraint forces found in systems using midspan restraints was found to be between the restraint force magnitudes for identical systems using third point and torsional restraint configurations.

In multiple purlin line systems, the total restraint force was not found to be the summation of the restraint forces of an equal number of single purlin line systems. The percent restraint force developed in a six purlin line system was found to be about 15% to 20% less than the restraint force developed in an identical two purlin line system. Further, it was found that restraint forces found in multi-span systems are less than those in an equivalent single span system with the same number of purlin lines.

Failure loads predicted using the local buckling provisions of the AISI specification and the constrained bending assumption were found to over estimate the actual failure loads by as much as 25%. The failure loads of systems with third point restraint configurations were found to be higher than the failure loads of systems using other configurations.

It was also found that the strength of a system is affected by the inclination of the edge stiffener with respect to the horizontal. However, essentially the same failure loads resulted when edge stiffeners were inclined between 75^0 and 90^0 with respect to the horizontal.

From the above, it is concluded that to achieve the

maximum capacity of roof systems, purlins with edge stiffeners inclined at 75^0 or greater with respect to the horizontal and restrained laterally at one third points of the span should be used.

REFERENCES

1. Specification for the Design of Cold-Formed Steel Structural Members, American Iron and Steel Institute, Washington, D.C., September 3, 1980.

2. Ghazanfari, A., and Murray, T.M., "Simple Span Z-Purlin Tests with Various Restraint Systems", Fears Structural Engineering Laboratory, Report No. FSEL/MBMA 82-01, University of Oklahoma, Norman, Oklahoma, February, 1982.

3. Ghazanfari, A., and Murray, T.M., "Simple Span Z-Purlin Tests with various Restraint Systems -- Addendum". Fears Structural Engineering Laboratory, Report No. FSEL/MBMA 82-01A, University of Oklahoma, Norman, Oklahoma, November, 1982.

4. Curtis, L.E., and Murray, T.M., "Simple Span Z-Purlin Tests to Determine Brace Force Accumulation", Fears Structural Engineering Laboratory, Report No. FSEL/MBMA 83-02, University of Oklahoma, Norman, Oklahoma, July 1983.

5. Ghazanfari, A., and Murray, T.M., "Prediction of Lateral Restraint Forces of Single Span Z-Purlins with Experimental Verification", Fears Structural Engineering Laboratory, Report No. FSEL/MBMA 83-04, University of Oklahoma, Norman, Oklahoma, October, 1983.

6. Zetlin, L., and Winter, G., "Unsymmetrical Bending of Beams with and without Lateral Bracing", Proceedings of the American Society of Civil Engineers, Vol. 81, 1955, pp. 774-1 to 774-20.

7. Needham, J.R., "Review of the Bending Mechanics of Cold-Formed Z-Purlins", Department of Civil Engineering, University of Kansas, Spring 1981.

8. Elhouar, S. "Prediction of Lateral Restraint Forces for Z-Purlin Supported Roof Systems", A thesis in preparation to be submitted to University of Oklahoma, Norman. 1984-85.

9. Litle, W.A., et al "Structural Behavior of Small-

Scale Steel Models", Bulletin No. 10, American Iron and Steel Institute, April 1968.

10. Brennan, P.J., and Mandel, J.A., "Multiple Configuration Curved Bridge Model Studies", Journal of the Structural Division, ASCE, Vol. 105, No ST5, Proc. Paper 14585, May 1979, pp. 875-890.

11. Moncarz, P.D., and Krawinkler, H., "Theory and Application of Experimental Model Analysis in Earthquake Engineering", Report No. 50, The John A. Blume Earthquake Engineering Center, Department of Civil Engineering, Stanford University, June 1981.

12. Skoglund, V.J., "Similitude, Theory and Applications", International Textbook Company, Scranton Pennsylvania, 1967.

13. Johnson, Donald, "Private Communication," May 1984.